

Influencer Videos: Unboxing the Mystique

Prashant Rajaram*
Puneet Manchanda

June 2020

This Version: November 10, 2023

* Rajaram (prajaram@ivey.ca) is Assistant Professor of Marketing at the Ivey Business School, Western University, and Manchanda (pmanchan@umich.edu) is Isadore and Leon Winkelman Professor and Professor of Marketing, at the Stephen M. Ross School of Business, University of Michigan. The authors would like to thank David Jurgens, Mengxia Zhang, Eric Schwartz, Zhenling Jiang, Jun Li, Yiqi Li, Yu Song, the Marketing faculty and doctoral students at the Ross School of Business, seminar participants at Ivey Business School, University of Wisconsin-Madison, Singapore Management University, Bocconi University, National University of Singapore, University of Manitoba, Bank of Canada, Bass FORMS Conference 2021, AIM Conference 2021, ISMS Marketing Science Conference 2021, Joint Statistical Meeting 2021, KDD 2021, ISMS Doctoral Consortium 2022, MSI Webinar 2022, Workshop by Global Institute for AI and Business Analytics 2023 and JSM 2023 for their valuable comments and feedback.

Abstract

Influencer marketing has become a very popular tool to reach customers. Despite the rapid growth in influencer videos, there has been little research on the effectiveness of their constituent features in explaining video engagement. We study YouTube influencers and analyze their unstructured video data across text, audio and images using an “interpretable deep learning” framework that accomplishes both goals of prediction and interpretation. Our prediction-based approach analyzes unstructured data and finds that “what is said” in words (text) is more influential than “how it is said” in imagery (images) or acoustics (audio). Our novel interpretation-based approach is implemented after completion of model prediction by analyzing the same source of unstructured data to measure importance attributed to the video features. We eliminate several spurious relationships in two steps, identifying a subset of relationships which are confirmed using theory. We uncover novel findings that establish distinct associations for measures of shallow and deep engagement based on the dual-system framework of human thinking. Our approach is validated using simulated data, and we discuss the learnings from our findings for influencers and brands.

Keywords: *Influencer Marketing, Video Advertising, Social Media, Interpretable Deep Learning, Transfer Learning*

1. Introduction

Influencers have the capacity to shape the opinion of others in their network. They were traditionally celebrities (e.g., movie stars and athletes) who leveraged their expertise, fame and following in their activity domain to other domains. However, 95% of the influencers today, or “social media stars,” are individuals who have cultivated an audience over time by making professional content that demonstrates authority and credibility (O'Connor, 2017). The growth in their audience(s) has been in part attributed to the fact that influencer videos are seen as “authentic” based on a perception of high source credibility. The increasing popularity of social media stars has resulted in an exponential growth of the influencer marketing industry which is expected to reach a global valuation of \$22.2B in 2025 from \$9.7B in 2020 (Statista, 2023). There are now more than 18,000 influencer marketing agencies in the world that allow brands to partner with influencers to promote their products (Influencer Marketing Hub, 2022). These influencers primarily reach their audience(s) via custom videos that are available on a variety of social media platforms (e.g., YouTube, Instagram, and TikTok) (Brooks, 2020).

Despite the rapid emergence and growth of influencer videos, there is limited research on the effectiveness of their constituent features. Specifically, little is known about the impact of different video features across text, audio and images in building video engagement. In this paper, we investigate this by developing an “interpretable deep learning” framework that comprises two approaches – prediction followed by interpretation. We apply our framework to publicly available influencer videos on YouTube, the platform where influencers charge the most for a post (Klear, 2019; McClure, 2020). We use a random sample of 1620 videos scraped from 33 YouTube influencers (across 11 product categories) who obtain revenue from brand endorsements. Our engagement measures on YouTube are divided into measures of shallow engagement (System I) (likes or dislikes) and deep engagement (System II) (comments) which are motivated by Kahneman’s work on frames of intuitive and deliberate thinking respectively (Kahneman, 2003).

First, in the prediction stage, we use unstructured data across different modalities – text, audio and images – as input to independent deep learning models designed for each modality, and then predict engagement out-of-sample. As the analysis of unstructured data is computationally very demanding, we overcome this challenge using transfer learning methods. These methods also have another benefit in that they prevent overfitting. We then combine predictions from each model of unstructured data with structured features to study the relative importance of each source of data in predicting engagement. We supplement the results of the prediction approach using a multimodal approach that takes embeddings from unstructured data as input and captures interactions between modalities during the training process. Second, in the interpretation stage, we peek inside the machine learning “black box” to interpret the relationships that were captured between theory-based features and our measures of engagement during

the prediction stage. We do this by adapting the theoretical framework of attention capture and transfer from the print advertising literature (Pieters & Wedel, 2004) to our influencer video setting and develop a novel two-step approach to shortlist plausibly causal relationships while removing several spurious associations in each step.

We implement our novel two-step interpretation approach as follows. First, we find correlations between theory-based features and the importance measures attributed by our model to these features. Doing so allows us to identify whether features in text, audio or images play an important role in predicting engagement. However, some of these correlations may only be important sporadically, i.e., over some but not all occurrences of the features, and hence not significantly influence predicted engagement (details in Section 3.2). In the second step, we check whether there exist correlations between theory-based features and the engagement measures predicted by our model. However, some of these correlations may be confounded with unobserved features. Hence, we shortlist relationships that are correlated in both steps, and end up eliminating many spurious relationships. Thus, we identify a subset of relationships, which are more likely to have external validity, for further formal causal testing. We validate (confirm) the identified relationships using theory and the design of our interpretation approach using simulated data. We also demonstrate the superiority of our approach over commonly used benchmark feature selection approaches such as LASSO and Elastic Net.

Our prediction results demonstrate that unstructured data in text (captions/transcript) capture more variation in all the engagement measures than unstructured data in images (video frames) or audio. This shows that “what is said” in words is more influential than “how it is said” in imagery or acoustics for predicting video engagement. We also find that on average, unstructured data in the beginning of videos explain more variation in engagement than data in the middle or end of videos. This suggests that, on average, the beginning of a video is sufficient to influence viewers’ decision to engage with a video (by commenting, liking or disliking) without needing to view the remainder of the video. These findings empower influencers by providing them directions along which design efforts can be prioritized to have the highest likelihood of improvement in engagement.

Our results from the ex-post interpretation also uncover some interesting findings. First, we find that mentioning brand names, especially in the electronics and digital categories, in captions/transcript in the beginning or middle of a video is more often associated with an increase in importance directed to the brand name but a decrease in the sentiment of *deliberate* reactions (System II). A decrease in entertainment value from discussion of commercial/marketing content is likely driving this effect. We also find that an increase in size of human images (and packaged goods) in the video frames displayed in the beginning 30 seconds is associated with an increase (and decrease) in the sentiment of *intuitive* reactions (System I). This can be explained by the desire to socialize, engage and communicate with other

humans. Overall, our findings from ex-post interpretation are broadly consistent with findings on related domains in previous literature, but are also novel in their ability to distinguish between effects on shallow (System I) and deep (System II) engagement.

Our results and approach are relevant for multiple audiences. For academics, who may be interested in testing causal effects, our novel interpretation approach is able to identify a smaller subset of relationships for formal testing. For practitioners, we provide a general approach to the analysis of videos used in marketing that does not rely on time-consuming primary data collection and can be undertaken with secondary data. For influencers and marketers, our results provide a theory-based understanding of the association between video features and relevant measures of engagement.

Overall, this paper makes four main contributions. First, to the best of our knowledge, it is the first paper that rigorously documents the relative contribution of sources of unstructured data (text, audio and images) in influencer videos in predicting video engagement. Second, it develops an “interpretable deep learning” framework that trains unstructured data to make good out-of-sample *predictions* and then peeks inside the same trained model to *interpret* the captured relationships, thus not making a tradeoff between prediction and interpretation. Third, it adapts the attention transfer and capture framework from the print advertising (theory) literature for use in the influencer video setting to interpret relationships using secondary data. Our novel ex-post interpretation approach eliminates several spurious relationships and shortlists a smaller subset of relationships for theory-based validation and formal causal testing. A broader view suggests that our approach can also be adapted to the analysis of long-form videos across multiple domains (e.g., education and politics). Finally, it presents novel substantive findings that uncover distinct effects for measures of deep and shallow engagement which can be validated by theory.

The remainder of the paper is organized as follows. Section 2 discusses related literature while Section 3 details our theoretical frameworks and theory-based features. Section 4 describes the data, Section 5 details the models, and Section 6 discusses our interpretation approach. Section 7 discusses the results, and Section 8 validates the methodological approach. Section 9 concludes with a discussion of the managerial implications, limitations and directions for future research.

2. Related Literature

In this section, we review the literature on influencer marketing and unstructured data analysis (using deep learning) and describe how our work builds on it.

2.1 Influencer Marketing

The growing literature on influencer marketing has analyzed influencer marketing effectiveness across text, audio and video data. Influencer marketing literature that analyzes textual data has found that high

influencer expertise on sponsored blog posts is more effective in increasing comments below the blog if the advertising intent is to raise awareness versus increasing trial (Hughes et al., 2019). Zhao et al. (2020) study the audio transcript of live streamers on the gaming platform Twitch, and find that lower values of conscientiousness, openness and extraversion but higher values of neuroticism are associated with higher views. Leung et al. (2022) study influencer text posts on Weibo and find that an increase in brand mentions are associated with an increase in the post's informativeness and result in an increase in reposts.

Use of audio and video data in influencer marketing research has gained increasing prominence in recent years. Hwang et al. (2022) find that influencers on Instagram use a softer voice in sponsored videos which can help increase the sentiment in comments below the post. Cheng and Zhang (2023) find that sponsored videos on YouTube by beauty and style influencers lead to a loss in subscribers as compared to organic videos created by them, and similarly Chen et al. (2022) find that early brand disclosure in influencer videos on Bilibili is associated with a reduction in the sum of likes, comments and shares for the video. On TikTok, Yang et al. (2023) find that a product that is advertised in the most engaging parts of a video leads to higher sales, and Tian et al. (2023) find that an increase in followers leads to an increase in impressions. Lanz et al. (2019) study network effects on a leading music platform, and find that unknown music creators can increase their follower base by seeding other creators with less followers than creators who are influencers (with more followers). Huang and Morozov (2022) study influencers on Twitch and find that their sponsored streams result in a negative ROI for game publishers. Using a theory model, Pei and Mayzlin (2022) model the extent of the affiliation decision between the brand and the influencer, and show that when a consumer's prior belief about product-influencer fit is high, the brand affiliates completely with the influencer to maximize awareness and prevent a negative review. In our paper, we add to the literature on influencer marketing by focusing on the role of unstructured data—text, audio and images—in YouTube influencer videos in promoting video engagement.

2.2 Unstructured Data Analysis in Marketing via Deep Learning

The use of deep learning methods to analyze unstructured data in the marketing literature has gained increasing prominence in recent years due to its ability to capture complex non-linear relationships that help make better predictions on outcomes of interest to marketers. Marketing research on textual data has used combinations of Convolutional Neural Nets (CNNs) and Long Short-Term Memory Cells (LSTMs) to study various outcomes including sales conversion at an online retailer (Liu et al., 2019), whether Amazon reviews are informative (Timoshenko & Hauser, 2019), sentiment in restaurant reviews (Chakraborty et al., 2022) and restaurant survival (Zhang & Luo, 2022). Research on image data has also used CNNs but within more complex architectures such as VGG-16 to classify and label images (Hartmann et al., 2021; Zhang et al., 2021), Caffe framework to predict brand personality (Liu et al., 2020) and ResNet152 to predict product return rates (Dzyabura et al., 2023).

Deep learning on video data has also been discussed in the marketing literature. Engineered features have been extracted from images, audio or text of video data to study their relationship with various outcomes, such as product preference while shopping (Lu et al., 2016), project success on Kickstarter (Li et al., 2019), consumer sentiment on Instagram (Hwang et al., 2022), video completion of educational courseware (Zhou et al., 2021) and number of subscribers on YouTube (Cheng & Zhang, 2023). Transfer learning has also been applied on video data to find the most engaging parts of the video that increase product sales on TikTok (Yang et al., 2023). There has also been research that embeds information from different data modalities using deep learning methods to create unified multi-view representations. Combinations of structured data and text have been used to predict business outcomes (Lee et al., 2022), brand logo images and textual descriptions have been combined to suggest logo features for a new brand (Dew et al., 2022), car designs have been combined with ratings data to suggest new designs (Burnap et al., 2023), and unstructured data from TikTok videos has been embedded in lower dimensional space to use as a control variable (Tian et al., 2023).

The marketing literature has also documented a tradeoff between predictive ability and interpretability (Dzyabura et al., 2023; Liu et al., 2020; Liu et al., 2019). Specifically, deep learning models that use unstructured data as input predict outcomes well out-of-sample because they capture complex non-linear relationships within constituent features of unstructured data. However, they suffer from poor interpretability as the inner workings of these models are frequently a “black box.” On the other hand, deep learning models that use ex-ante handcrafted features as input obtain high interpretability of the captured relationships because one can observe a change in outcome for a unit change in a structured feature. However, they suffer from poor predictive ability because these handcrafted features do not capture all the underlying latent constructs. We avoid this tradeoff by developing an “interpretable deep learning” framework that accomplishes both goals of prediction and interpretation, and thus extend the work in prior literature. We explain this framework in Section 3.

3. Theoretical Frameworks

We explain our theoretical frameworks in 3.1 and 3.2, and describe our theory-based features in 3.3.

3.1 Interpretable Deep Learning Framework

Our interpretable deep learning framework is shown in Figure 1, where we use unstructured video data as input to a set of deep learning models that predict engagement with a video. Training deep learning models from scratch can be computationally very demanding and can lead to overfitting unless one has superior computational resources and millions of data points respectively (typically only available to big companies). Hence, to circumvent these issues, we use a transfer learning approach. First, we use a base (deep-learned) model (for each source of unstructured data - text, audio or images) that has been pre-

trained in previous machine learning literature on a separate task with millions of observations at a very high computational cost. On top of the base models, we implement novel customizations and design architectures that help with prediction (and ex-post interpretation). We then finetune the models to capture the relationship between different sources of unstructured video data (text, audio and images) in our sample and our measures of engagement. This process of transfer learning also aids in interpretation because these models have pre-learned basic features for text, audio and images over millions of observations. Hence, during finetuning, our transfer learned models can easily capture word context, sound classes and image characteristics in our sample of influencer videos.

As we use unstructured video data as input (and not handcrafted features), we achieve predictive ability. After completing prediction, we implement interpretation by “peeking” inside the trained model to uncover the captured relationships. We explain the framework behind interpretation in 3.2.

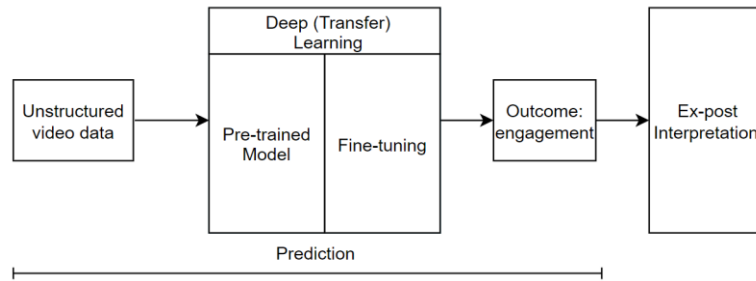


Figure 1: Interpretable Deep Learning Framework

3.2 Ex-Post Interpretation Framework

To the best of our knowledge, there is no extant theoretical framework that links the impact of influencer videos to their constituent features. In this paper, we propose such a framework that is an adaption of the theoretical framework describing attention capture and transfer in print advertising in Pieters and Wedel (2004). Their framework describes the effect of bottom-up (automatic) factors and top-down (volitional) factors that can affect attention to ad features. In primarily “entertainment commerce” platforms, such as YouTube and TikTok, bottom-up attention (or saliency-based attention) is more likely to be exhibited by viewers compared to top-down attention which is more volitional and more commonly occurs in search driven product markets (Yang et al., 2023). Viewers primarily come to such platforms for entertainment (Google, 2016), and salient features in videos are more likely to grab viewer’s bottom-up attention. These salient features could be in either text, audio or images. The part of the framework of Pieters and Wedel (2004) that is directly relevant for our influencer video setting is shown in Figure 2.

The figure illustrates the “bottom-up attention capture” conceptual model, where a stimulus such as the size of a brand logo in a print ad affects the reach of prints ads via the mediating effect of visual attention to the stimulus. We describe our approach to implement their framework in the bottom half of Figure 2. The stimuli (or features) in our setting comprise the presence of text features, duration of audio

features or size of image features in influencer videos (Box A) (detailed in Section 3.3). We capture *model attention* (not viewer visual attention) to these features (Box B) using independent deep learning models for each source of unstructured data (text, audio or images). These models are more attentive to those features in videos that explain better variation in engagement (Box C)¹ (Selvaraju et al., 2017; Vashishth et al., 2019). Hence in our setting, the effect of a feature on engagement is mediated by the effect of model attention to the feature. By acting as a mediator, model attention (attributed to a feature) is theoretically a necessary condition for the feature to explain variation in predicted engagement. This is similar to the setting for print ads where visual attention to brand related features in an ad is a necessary condition for obtaining effects of brand communication (Pieters & Wedel, 2004). We capture this necessary condition in Step 1 of our analysis by finding correlations between the feature (Box A) and the *importance* (attention) attributed to the feature (Box B) while training our models. By studying these correlations, we are able to identify whether certain features play an important role in predicting engagement.

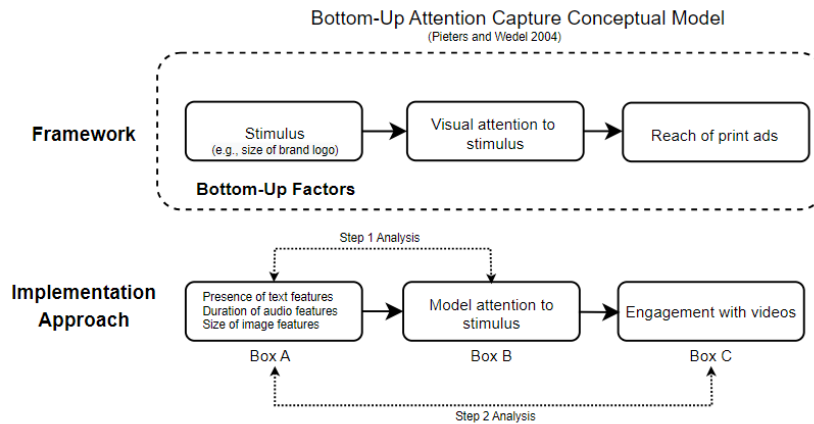


Figure 2: Ex-Post Interpretation Framework

Note that an increase in attention is only a necessary condition and not a sufficient condition for the feature to have a significant effect on predicted engagement. This is because deep learning models may attribute importance to a feature over only some of its occurrences and not all of its occurrences (either within or between observations) in the data. In other words, some features can be sporadically important and still result in a significant association between that feature and the attention attributed to it. This is because that feature can, on average, be more important than other features that are never important. In the setting for print ads, these are akin to stimuli (features) that occasionally catch the viewer’s eye but don’t causally affect brand communication. Such sporadically important features are *less* likely to have a significant association with predicted engagement as compared to frequently important

¹ The framework in Pieters and Wedel (2004) uses eye-tracking studies to measure visual attention. We complement this stream of work by analyzing secondary data, and introduce the concept of *model attention* from the machine learning literature to the marketing literature. Our approach can be applied on public videos that potentially engage millions of viewers over many minutes of viewing, as opposed to the small number of viewers in conventional lab or field studies. It is also important to note that model attention is not independent of eye tracking attention, and extant research in machine learning has found that they have a statistically significant correlation (Selvaraju et al., 2017).

features. This is because deep learning models are theoretically designed to rely more on frequently important features than sporadically important (or never-important) features to predict the outcome. In order to identify and remove sporadically important features, we implement Step 2 of the analysis where we capture correlations between the features (Box A) and *predicted* engagement measures that have been returned by our deep learning models (Box C). We use predicted engagement (and not observed engagement) as the dependent variable. This is because it has been theoretically influenced by the importance measures, and hence using it in Step 2 will be directly comparable with the analysis in Step 1 that uses (estimated) importance measures as the dependent variable (see equations in Section 6).

In Step 2 of the analysis, some of the features can be spuriously correlated with predicted engagement without the necessary condition of the mediating effect of an increase in attention. This would suggest presence of an unobserved confounding factor that is correlated with both the feature and predicted engagement. Hence, we find relationships at the intersection of Step 1 & 2. This is visually illustrated using a Venn diagram in Figure 3 (its detailed implementation is discussed in Section 6).

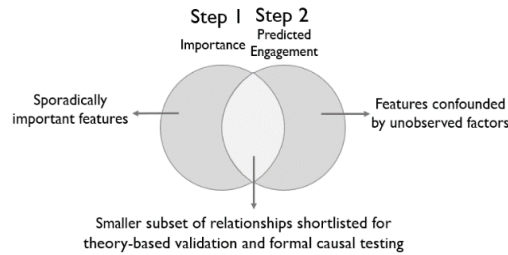


Figure 3: Implementation of Ex-Post Interpretation

We remove sporadically important features from the left side and confounded features from the right side of the Venn diagram. We thus identify features (Box A) that result in both an increase in attention (Box B) and a change in predicted engagement (Box C). However, deep learning models are known to be “brittle” as they can randomly converge to a local optimum. Hence, we run each model multiple times (details in Section 7), to mitigate concerns of brittleness while identifying these relationships. Despite doing so, it is important to note that neither Step 1 nor Step 2 are sufficient conditions to identify causal features. This is because our approach can potentially also shortlist relationships that are spuriously correlated across both steps by coincidence. Overall, our approach does not guarantee that *all* the relationships at the intersection of Step 1 and 2 are causal, but by removing spurious associations across both steps, it identifies a subset of relationships that are more likely to contain causal relationships. Given this subset, we then apply theory to validate whether the relationships (at the intersection) are plausibly causal. We detail this theory in Section 3.3.

3.3 Theory-based Features

We would like to choose features that can be locally identified (as salient regions) within text, audio or images so that they can be used within the theoretical framework of Figure 2. For example, a person in an

image can be locally identified but the brightness of an image refers to the entire image and is not a local aspect of an image (Dzyabura et al., 2023; Li et al., 2019; Zhang et al., 2021). We narrow our focus to those local features which can drive a change in the sentiment of engagement as guided by theory (in past literature) and which are also likely to be of interest to marketers and brand partners. We elaborate on these features below and summarize the corresponding theory-based expectations in Table 1.

3.3.1 Presence of text features

Viewers like viewing ads which have high entertainment value and low informational value (Wilbur, 2016; Woltman Elpers et al., 2003). Similarly, viewers view influencer videos for their entertainment value (Landsberg, 2021). As discussed earlier, features in entertaining videos can activate bottom-up attention which can affect engagement with the video. Brand mentions (in captions/transcript) in influencer videos are features that can lower entertainment value and increase informational value as discussion surrounding brand disclosure is typically commercial in nature (Tellis et al., 2019). This in turn can lead to a reduction in the persuasiveness of the message (Teixeira et al., 2010; Tellis et al., 2019), which can manifest as a reduction in (positive) sentiment for the video. On the other hand, a competing view suggests that increase in informational value may complement the entertainment value of video content, educate viewers about the brand and increase viewers' trust in the brand (Leung et al., 2022). This can be associated with an increase in (positive) sentiment for the video.

Use of emotional words has been found to be positively associated with engagement measures such as number of shares, comments and likes for Facebook ad messages or New York Times articles (Berger & Milkman, 2012; Lee et al., 2018). This is because emotional words are typically tied to a brand's personality and help increase persuasiveness of the message (Lee et al., 2018). Such words can also evoke high arousal leading to an excitatory state (Berger & Milkman, 2012). Hence, emotional words can be associated with an increase in (positive) sentiment for the video. A competing view suggests that use of emotional words is often associated with disingenuous persuasion or insincerity which is commonly found in fake news stories (Bakir & McStay, 2018; Guo et al., 2019). This suggests that use of emotional words can be associated with a decrease in (positive) sentiment for influencer videos.

Given these contrasting set of findings in prior literature on the effect of brands and emotional words, their association with the sentiment for influencer videos is unclear ex-ante.

3.3.2 Duration of audio features

Music in ad videos has been found to reduce irritation towards the ad (Pelsmacker & Van den Bergh, 1999). Furthermore, use of music without voiceover can have a stronger effect than use of music with voiceover on memory for brand names (Alexomanolaki et al., 2007). Hence, an increase in the duration of music without voiceover can be expected to be associated with an increase in (positive) sentiment.

Unstructured data	Features in unstructured data	Theory	Representative Source	Expected change in sentiment of engagement
Text: Captions/ Transcript	Presence of brand names	Brand mentions may lower entertainment value and decrease persuasiveness of message. Brand mentions may increase informational value and increase viewers' trust in the brand.	Tellis et al. 2019; Teixeira et al. 2010 Leung et al. 2022	Ambiguous
	Presence of emotional words	Emotional words are tied to a brand's personality, evoke high arousal and increase message persuasiveness. Emotional words are associated with disingenuous persuasion or insincerity and signal fakeness.	Lee et al. 2018; Berger & Milkman 2012 Bakir & McStay 2018; Guo et al. 2019	Ambiguous
Audio	Duration of music	Music in ad videos reduces irritation towards the ad.	Pelsmacker & Van den Bergh 1999	Positive
	Rapid speech	Rapid speech is associated with being more knowledgeable and an increase in watch time. Change in pace of influencer's voice grabs viewer attention.	Peterson et al. 1995; Guo et. al. 2014 Beck 2015; Jennings 2021	Ambiguous
Images: Video Frames	Size of humans	Human images increase desire to socialize, engage and communicate.	Xiao and Ding 2014; Hartmann et al. 2021; To & Patrick 2021	Positive
	Size of packaged goods	Packshots (which focus on a product and not humans) decrease desire to socialize, engage and communicate.	Hartmann et al. 2021	Negative
	Size of animals	Ads featuring animals are more likeable.	Biel & Bridgwater 1990; Pelsmacker & Van den Bergh 1999	Positive
	Emotional expressions of joy and surprise	Joy and surprise in internet videos ads concentrate attention and retain viewers for longer time periods. Joyous faces are associated with decrease in retweets but are not associated with likes on Twitter or Instagram. Surprise exhibited by instructors in educational videos has no dominant directional effect on video watch time, as it depends on contextual factors and topics discussed	Teixeira et al. 2012 Li & Xie 2020 Zhou et al. 2021	Ambiguous

Table 1: Theory-based stimuli and expectations

Past research has found that fast speakers are rated as being more knowledgeable and more effective salespersons than slow speakers (Peterson et al., 1995). Similarly, research on educational videos has found that faster speaking rate of instructors is associated with an increase in watch time (Guo et al., 2014). On the other hand, linguists who have analyzed influencer videos find that a change in pace, and not rapid speech, is what grabs viewer attention (Beck, 2015; Jennings, 2021). This is not necessarily surprising given that one of the primary goals of influencers is to “entertain” viewers (Landsberg, 2021) which is further complemented with sales pitches. Given these contrasting results in prior research, it is unclear whether rapid speech can be expected to have an association with sentiment for influencer videos.

3.3.3 Size of image features

Human faces have been preferred in print ads (Xiao & Ding, 2014) and they have been associated with an increase in likes, comments and shares on social media posts (Li & Xie, 2020; Yang et al., 2023). The reason for this positive association can be explained by the desire to socialize, engage and communicate with other humans (To & Patrick, 2021; Xiao & Ding, 2014). Moreover, in influencer videos, the influencer is often demonstrating something to a viewer with the help of their hands, such as the details of a product. We expect this action of the influencer to further aid in engaging the viewer and improve sentiment for the video. In summary, we can expect the size of the whole human (influencer) in the video, including the area near their hands, to be associated with an increase in (positive) sentiment.

Similarly, Hartmann et al. (2021) find that images of brand selfies and packshots are associated with a decrease in likes on Instagram as compared to consumer selfies because of a decrease in desire to engage with non-human images. Importantly, in influencer videos, packaged goods are objects that can draw attention in the video since influencers use them as part of a demonstration (e.g., unboxing video, tutorial, etc.). Hence, we expect an increase in size of packaged goods to be associated with a decrease in (positive) sentiment of engagement. Furthermore, just like videos featuring humans, ads featuring animals have been found to be more likeable and have an extremely low irritation score (Biel & Bridgwater, 1990; Pelsmacker & Van den Bergh, 1999). Hence, we expect an increase in size of animals in influencer videos to also be associated with an increase in (positive) sentiment for the video.

Facial expressions such as joy and surprise in internet video ads have been found to concentrate attention and retain viewers for longer periods of time (Teixeira et al., 2012). On the other hand, joyous (happy) faces have been found to be associated with fewer retweets on Twitter, and have been found to have *no* significant association with likes on Twitter or Instagram (Li & Xie, 2020). Similarly, surprise exhibited by instructors in educational videos has been found to either increase or decrease the likelihood of video watch time as its effect varies based on contextual factors and topics discussed (Zhou et al., 2021). Given these set of contrasting results on the effect of facial expressions, there is ambiguity about their association with the sentiment towards influencer videos.

4. Data

We focus on influencer videos on YouTube, the platform where influencers charge the most for a post due to the higher production cost of long-form videos which are more common on YouTube than other social media platforms (Klear, 2019; McClure, 2020). Long-form videos are different from conventional ad videos in at least three ways (a) they can (and almost always do) contain information unrelated to the sponsoring brand (e.g., gaming videos, vlogs, etc.) (b) are much longer than a standard 30 sec TV ad, and (c) can be interrupted by traditional ads on YouTube.

We focus on 110 influencers identified by Forbes in February 2017 (O'Connor, 2017). Specifically, we look at 10 influencers in each of 11 product categories (Beauty, Entertainment, Fashion, Fitness, Food, Gaming, Home, Parenting, Pets, Tech & Business, Travel). These influencers² are the top performers in their category, obtain revenue from brand endorsements and post mostly in English across Facebook, YouTube, Instagram and Twitter. In order to create our final data sample, we first exclude influencers who do not have a YouTube channel. We also use the industry threshold of 1000 followers for a person to be classified an influencer (Maheshwari, 2018) and also exclude one atypical influencer with more than 100M followers. Furthermore, we short-list those influencers who have posted at least 50 videos so that we can capture sufficient variation in their activity, which leaves us with 73 influencers.

Our selection criteria allow us to focus on popular YouTube influencers who primarily make content for adults, have between 1000 and 100M subscribers which is typical of the range of subscribership for influencers on YouTube, and posted only pre-recorded videos. From this pool, we randomly choose 3 influencers per category, which gives a total of 33 influencers who can be divided based on the number of subscribers as follows: 1000 to 10K (2), 10K to 100K (6), 100K to 1M (7), 1M to 10M (13), and 10M+ (5). We use the YouTube Data API v3 to scrape the title and posting time of all videos posted by these 33 influencers till October 2019 and this totals 32,246 videos.³ We randomly choose 50 public videos for each influencer so that we have a balanced sample of 1650 videos whose unstructured data (text, audio and images) is computationally feasible to analyze (details in Section 7.1). Excluding videos in which likes, dislikes or comments were disabled by the influencer(s) leaves us with 1620 videos and we scrape all associated data that was publicly available in November 2019.

First, we investigate whether the influencers in our sample comply with the US Federal Trade Commission (FTC) guidelines to disclose sponsorship early in the video using words such as “ad”, “sponsor”, etc. (FTC, 2020). We examine the captions/transcript in the beginning (and middle) of the video and find that only 1% of videos make such disclosures which suggests little compliance with the guideline. Next, we detail the input data for our models in 4.1 and discuss our outcome measures in 4.2.

4.1 Input Data

We list the unstructured data which we supply as input to our models (described in Section 5) in Table 2. Text data comprise the title of the video, description below the video and captions/transcript of the video. For the video description, a maximum of 160 characters are visible in Google Search and even fewer characters are visible below the video before the ‘Show More’ link (Cournoyer, 2014). Hence, we truncate each description to the first 160 characters (160 c) as it is more likely to contribute to any

² The criteria used by Forbes to identify these influencers include total reach, propensity for virality, level of engagement, endorsements, and related offline business.

³ Our usage of this data falls within the ambit of YouTube’s fair use policy (YouTube, 2020).

potential association with our outcomes. Captions are only present in 74% of videos, and for those videos without a caption, we use Google’s Cloud Speech-to-Text Video Transcribing API to transcribe the audio file to English. We also use the raw audio data in addition to captions/ transcript to capture acoustic information (e.g., music). Image data comprise thumbnails and image frames captured at the conventional sampling frequency of one fps (frame per second) (Yang et al., 2023; Yue-Hei Ng et al., 2015). These frames are at a good resolution of 135x240 pixels that is both visually clear and feasible to analyze.

Type	Class	Features
Unstructured Data	Text	Title
		Description (first 160 characters)
		Captions or Transcript (divided into 30 sec segments)
	Audio	Audio file (divided into 30 sec segments)
	Images	Thumbnail
Video Frames (divided into 30 sec segments) at one fps		
Structured Features	Fixed Effects	Influencer Fixed Effects (33)
	Length	Video Length (min)
	Tags	Number of video tags (see Google (2020) for details)
	Playlist Information	Number of playlists the video is a part of
		Average position in playlist
		Average number of videos on all the playlists the video is a part of
	Time based covariates	Time from upload time to scrape time
		Year of upload (2006 to 2019)
		Time between uploads: Given and preceding influencer video in master list
		Time between uploads: Given and succeeding influencer video in master list
		Rank of video among all videos of the influencer in the master list
		Day fixed effects (7) in EST
		Time of day fixed effects in intervals of 4 hours from 00:00 hours EST (6)
Captions Indicator	Indicator of whether video has closed captions	
Structured features from full description	Total number of URLs in description	
	Indicator of Hashtag in description	

Table 2: Input data – Unstructured data and structured features

For the unstructured data in captions/transcript, audio and video frames, we divide the data into segments of 30 seconds (e.g., for a 10 minute video, we have 20 segments) for two reasons. First, the minimum duration of video content that needs to be viewed for an impression to be registered is 30 seconds (Parsons, 2017) which makes this an adequate threshold. Second, higher computational costs associated with analyzing raw unstructured data in our individual deep learning models require us to restrict data size to a feasible amount (details in Section 5.1). Note that for image frames, we extract 30 frames from each 30 second clip, at one fps.

We also list the structured features that we supply as input in Table 2. These comprise fixed effects for the influencer (channel), video length, number of tags, features for playlist information, time-based-features and an indicator for whether captions are available for the video. We create two additional structured features from the *complete* description (as it is not supplied as input to the Text Model). They

comprise total number of URLs in description and an indicator for hashtag in description, and these are important as they can lead the viewer away from the video.

4.2 Outcome Variables

The top three ways of measuring influencer marketing success in the industry are conversions, engagement and impressions (Influencer Marketing Hub, 2022). Unfortunately, conversion data are not publicly available, and the measure of impressions (views) can be confounded with the impact of YouTube's recommendation algorithm (explained ahead). Hence, we focus on engagement, which is important to brands to not only measure campaign success but also to ex-ante decide on a collaboration (Influencer Marketing Hub, 2022). Furthermore, measures of engagement (such as number of comments, likes, and sentiment of comments) have been linked with sales and profitability in related contexts such as brand managed social media communities (Goh et al., 2013; Gomez, 2021; Rishika et al., 2013).

We construct our measures of engagement using the dual-system framework – System I and System II – theory of human thinking (Kahneman, 2003).⁴ System I thinking corresponds to more automatic and intuitive reactions that require less thought. This is captured by measures of shallow engagement that include a count of thumbs up / like (YouTube, Facebook, Instagram, etc.), thumbs down / dislike (YouTube and TikTok) or retweets (Twitter) that require little effort and can be accomplished with a simple click of a button (Social Media Week, 2017). System II thinking captures more effortful, conscious and deliberate reactions that require more thought. This is captured by measures of deep engagement that include a count of comments (YouTube, Facebook, Instagram, Twitter, etc.) which require more effort as it involves typing a response (Dwoskin, 2021).

Extant literature in marketing or extant metrics in the industry have typically not distinguished between measures of shallow or deep engagement likely because these measures are always highly correlated (Gogolan, 2022; Hartmann et al., 2021; Hughes et al., 2019; Lee et al., 2018). For example, across our sample of 1620 videos there is high correlation between log views and log (comments+1) at 0.91, between log views and log (likes+1) at 0.95 and between log views and log (dislikes+1) at 0.92 (we add 1 to avoid log of 0). An added concern in social media platforms is the confound of the recommendation algorithm that may be correlated with these measures of engagement. For example, YouTube's algorithm analyzes watch history and video content to recommend videos with higher expected watch time for a viewer, which should be highly correlated with total views for the video (Covington et al., 2016). We overcome the two problems of (1) high correlation between measures of shallow and deep engagement and (2) the confound of the YouTube algorithm, in the following manner. We construct engagement measures that control for the number of views, and hence capture shallow or

⁴ These frames of thinking have also been introduced in prior research in related contexts such as peripheral and central routes of persuasion (Petty & Cacioppo, 1986) and heuristic and systematic modes of information processing (Chen & Chaiken, 1999).

deep engagement *conditional on viewing a video*. This results in unique constructs that are not highly correlated with each other or with views and are also dominated by distinct underlying factors (see 4.2.3). The absence of high correlation with views indicates that our measures are unlikely to be confounded with the algorithm. Similarly, any promotional activities by brands to increase the reach of influencer videos will result in an increase in views, but are unlikely to affect our measures of engagement.

We next explain our engagement measures through the prism of engagement level and the corresponding sentiment of engagement.

4.2.1 Engagement Level

We develop unique measures to capture the shallow and deep engagement level: (a) “Thumbsability”:
 $\frac{\#likes + \#dislikes}{\#views}$, which measures the level of shallow engagement and (b) “Commentability”:
 $\frac{\#comments}{\#views}$, which measures the level of deep engagement. Thumbsability is a measure of the number of thumbs up (likes) or thumbs down (dislikes) conditional on viewing the video. As this requires less thought and can be accomplished with a simple click (Social Media Week, 2017), it captures more automatic, intuitive and less deliberate reactions. On the other hand, commentability is a measure of number of comments conditional on viewing the video. As typing a response is more effortful and requires more thought (Dwoskin, 2021), this measure captures more conscious and deliberate reactions. By scaling each engagement measure by a count of views, we develop unique constructs that are not highly correlated with each other (see 4.2.3). As the two measures of engagement level are exponentially distributed, we take their natural log, and add 1 to avoid computation of log (0): $\log \text{ thumbsability} = \log \left(\frac{\text{likes} + \text{dislikes} + 1}{\text{views}} \right)$, and $\log \text{ commentability} = \log \left(\frac{\text{comments} + 1}{\text{views}} \right)$. Log thumbsability has a median of -3.78 (or approximately 228 likes or dislikes per 10K views) and log commentability has a median of -6.21 (or approximately 20 comments per 10K views).

4.2.2 Sentiment of Engagement

Past work has found that the visual and verbal components of advertising can have an effect on attitude towards the ad which in turn can have a direct effect on overall brand attitude, including attitude towards purchasing and using the product (Mitchell, 1986). Moreover, the sentiment of user generated content on brand managed social media communities has also been linked with sales (Goh et al., 2013). Hence, brands can benefit from understanding viewer attitude or sentiment towards videos as it can act as a proxy for sales. We develop unique measures to capture the sentiment of shallow and deep engagement: (a) “Likeability”:
 $\frac{\#likes}{\#dislikes}$, which measures the sentiment of shallow engagement and (b) “Loveability”:
which measures the sentiment of deep engagement by capturing the sentiment in comments using Google’s Natural Language API. Likeability measures the probability of a viewer to like rather than

dislike a video. Higher the value of likeability, more positive is the sentiment of shallow engagement. As the measure is a ratio of two different measures, it is not highly correlated with the other outcome variables (see 4.2.3). As done before, we take the log of likeability and add 1 to avoid computation of log (0) or log(∞): $\log \text{likeability} = \log \left(\frac{\text{likes}+1}{\text{dislikes}+1} \right)$, and it has a median of 3.99 (or 54 likes per dislike).

We capture loveability by measuring the average sentiment expressed in the Top 25 comments below a video. Note that comments below a video are by default sorted as ‘Top comments’ and not ‘Newest first,’ using YouTube’s proprietary ranking algorithm.⁵ We do not measure the sentiment in the replies to each of the Top 25 comments because sentiment expressed in the reply is likely to be sentiment towards the comment and not sentiment towards the video. We capture the sentiment in comments using Google’s Natural Language API which is pre-trained on a large document corpus, supports 10 languages, and is known to perform well in sentiment analysis on textual data (including emojis) in general use cases (Hopf, 2020; Li & Xie, 2020). For comments made in a language not supported by the API, we use the Google Translation API to first translate the comment to English, and then find its sentiment. The sentiment provided is a score from -1 to $+1$ (with increments of 0.1), where -1 is very negative, 0 is neutral and $+1$ is very positive. We calculate the sentiment of each comment below a video up till a maximum of 25 comments, and then find the average sentiment score. As a robustness check, we scrape and then use Top 50 or 100 comments for a random sample of 66 videos (2 videos per influencer) and also explore use of decreasing weights instead of a simple average. We find that the sentiment calculated using any of these measures is highly correlated with a simple average of Top 25 comments ($\rho \geq 0.88$).

We use the median value (0.34) of the distribution of average sentiment score as a cut-off to divide loveability into two buckets – “positive” and “not positive (neutral or negative).” We convert loveability into a discrete measure instead of retaining a continuous measure because sentiment cannot be measured objectively using a continuous measure. There can be minor variations based on the choice of the API (or algorithm/human coder). Hence, by using a discrete measure, we are able to create a more objective measure of sentiment in comments, which is consistent with the approach used in prior research (Goh et al., 2013; Li & Xie, 2020). We also assume that if viewers choose to not post comments below a video (though comment posting is not disabled), then the sentiment towards the video is neutral.

4.2.3 Summary of outcome variables

We have a total of three continuous outcomes and one binary outcome that are summarized in Table 3a. We find that the average magnitude of the Pearson correlation coefficient between each of the four outcome variables is 0.28, with the individual values shown in Table 3b.

⁵ Higher ranked comments (lower magnitude) have been empirically observed to be positively correlated with like/dislike ratio of comment, like/dislike ratio of commenter, number of replies to the comment and time since comment was posted (Dixon & Baig, 2019). Moreover, a tabulation shows that 99% of comments are made by viewers and not the influencer (who owns the channel) and hence we do not separate the two.

We have a total of three continuous outcomes and one binary outcome that are summarized in Table 3a. We find that the average magnitude of the Pearson correlation coefficient between each of the four outcome variables is 0.28, with the individual values shown in Table 3b. This indicates that the measures on average are not highly correlated with each other. We also carry out a Principal Component Analysis (PCA) on our outcome measures (and views), as shown in Table 3c, and find that each measure loads heavily (≥ 0.83) on a distinct underlying construct. This provides further evidence that each outcome variable is capturing unique information: {deep or shallow} x {engagement level or sentiment}.

	Deep Engagement	Shallow Engagement
Engagement Level	Commentability: $\frac{\#comments}{\#views}$	Thumbsability: $\frac{\#likes+\#dislikes}{\#views}$
Sentiment of Engagement	Loveability: Positive or Not Positive	Likeability: $\frac{\#likes}{\#dislikes}$

Table 3a: Summary of outcome variables

	Log thumbsability	Log commentability	Log likeability	Loveability	Log views
Log thumbsability	1				
Log commentability	0.67	1			
Log likeability	0.53	0.14	1		
Loveability	0.01	-0.15	0.15	1	
Log views	0.18	0.04	0.43	-0.21	1

Table 3b: Correlation between variables

	Factor 1	Factor 2	Factor 3	Factor 4	Factor 5
Log thumbsability	0.45	0.32	0.07	0.02	0.83
Log commentability	0.96	0.04	0.00	-0.09	0.28
Log likeability	0.05	0.94	0.24	0.10	0.23
Loveability	-0.07	0.08	-0.11	0.99	0.01
Log views	0.01	0.21	0.97	-0.12	0.05

Table 3c: Factor Loadings from a PCA of variables

5. Model

In this section, we discuss our two main modelling approaches: (a) The Combined Model that combines information from individual (transfer learned) deep learning models for each modality of unstructured data (text, audio and images), and (b) the Multimodal Model that uses embeddings from each modality of unstructured data in an end-to-end training approach. We summarize these approaches in Table 4. We discuss our choice of the individual deep learning models in 5.1. We describe how we combine information from all the individual models in 5.2. We contrast this with a multimodal approach in 5.3.

Model	Approach	Advantage	Disadvantage	Input Data
Combined Model	Combine individual models for each source of raw unstructured data	Captures complex interactions between raw unstructured data in each modality and the outcome	Higher computation time of individual models; Loss of information from not capturing interactions among latent dimensions of different modalities of data	30 seconds in beginning, middle and end (Results in 7.1.2)
Multimodal Model	One model using embeddings from each source of raw unstructured data	Lower computation time; Captures interactions among latent dimensions of different modalities of data during training	Loss of information from using embeddings instead of raw unstructured data	(a) 30 seconds in beginning, middle and end (Results in 7.1.3) (b) 30 second segments over <i>entire video</i> (Results in 8.1)

Table 4: Summary of Modelling Approaches

5.1 Individual Models

We analyze text data using Bidirectional Encoder Representation from Transformers (BERT) a high performing NLP model that borrows the Encoder representation from the Transformer framework (Devlin et al., 2018). The model is pre-trained using Book Corpus data (800M words) and English Wikipedia (2,500M words) to predict words and sentences over four days using four Tensor Processing Units. We fine-tune the BERT model on our data sample to capture the association with our four outcomes. As BERT uses a *self-attention* mechanism, it allows the model to simultaneously identify importance (attention weights) associated with all words in text. We interpret these attention weights during ex-post interpretation. We provide details on how we operationalize this framework in Online Appendix A.

We analyze audio data using the pre-trained YAMNet model (Pilakal & Ellis, 2020), and customize it with an additional Bidirectional LSTM (Bi-LSTM) layer and an attention mechanism. The model is pre-trained on AudioSet data (which has more than 2M 10-sec YouTube audio segments) (Gemmeke et al., 2017). We fine-tune the Audio model on our data sample to capture the association with our four outcomes. The attention mechanism, which we adopt from the literature on neural machine translation (Bahdanau et al., 2014), helps the model capture the relative importance (attention) weights between sound moments. We interpret these attention weights during ex-post interpretation. We provide details on how we operationalize this framework in Online Appendix B.

We analyze individual images using the high performing and popular image model – VGG-16 that has been pre-trained on 1.2M images from the ImageNet dataset (Hartmann et al., 2021; Zhang et al., 2021). For analyzing video frames, we combine the output from each VGG-16 model with a Bi-LSTM, which is known to be one of the best performing architectures at capturing sequential information from video frames (cf. Yue-Hei Ng et al. (2015)). We fine-tune the Image model on our data sample to capture

the association with our four outcomes. We ex-post identify the salient areas of images that are associated with an outcome through gradient-based activation maps (cf. Selvaraju et al., 2017) and modify this such that positive (negative) gradients corresponding to regions that are positively (negatively) associated with continuous outcomes and the predicted class of the binary outcome. We provide details on how we operationalize the model and find gradients in Online Appendix C, and we analyze these gradients during ex-post interpretation. While negative gradients identify areas that are negatively associated with an outcome, negative attention weights in the Text and Audio model identify areas that do not have an association. We do not use an “attention weight” based approach here to find salient areas because that would be computationally very expensive over a 135x240 pixel frame for 30 frames. The gradient approach accomplishes the same objective more efficiently.

Note that all the design architectures of our individual deep learning models have been validated in prior machine learning literature for their ability to explain model predictions by assigning importance (attention/ gradients) to features (Selvaraju et al., 2017; Vashishth et al., 2019). We train the individual models on 30 seconds of raw unstructured data from the beginning, middle or end of a video, and not the entire video due to computational constraints (e.g., it takes 432 hours to analyze images in our sample using a 48GB GPU – more details in 7.1).

5.2 Combined Model

We use equation (1) to combine information from unstructured data and structured features. Information from unstructured data is included by using the predicted outcome values \hat{Y}_{it} for video t by influencer i generated by supplying 30 seconds from each part (beginning, middle or end) of each source of unstructured data (listed earlier in Table 2) to the appropriate individual model discussed in 5.1. The structured features, X_{it} , (listed earlier in Table 2) are supplied as an additional input to the equation. We test different models, g , to combine information from all these sources of data and capture any potential interactions between them. Equation (1) is shown below,

$$Y_{it} = g \left(\begin{array}{c} X_{it}, \hat{Y}_{it}^{Title}, \hat{Y}_{it}^{Description (first 160 c)} \\ \hat{Y}_{it}^{Captions-Transcript (beginning)}, \hat{Y}_{it}^{Captions-Transcript (middle)}, \hat{Y}_{it}^{Captions-Transcript (end)} \\ \hat{Y}_{it}^{Audio (beginning)}, \hat{Y}_{it}^{Audio (middle)}, \hat{Y}_{it}^{Audio (end)} \\ \hat{Y}_{it}^{Thumbnail}, \hat{Y}_{it}^{Video Frames (beginning)}, \hat{Y}_{it}^{Video Frames (middle)}, \hat{Y}_{it}^{Video Frames (end)} \end{array} \right) + \epsilon_{it} \quad (1)$$

where Y_{it} is the observed outcome for video t by influencer i , g is the combined model used and ϵ_{it} is the error term. We test the performance of seven different combined models that are known to predict well out-of-sample. They comprise four linear models – OLS, Ridge Regression, LASSO and Elastic Net, and three non-linear models – Deep Neural Net, Random Forests and Extreme Gradient Boosting. Our choice of these combined models is guided by their high predictive performance in machine learning literature.

The advantage of this approach is that it uses predictions from tailor-made models for each source of unstructured data which are fine-tuned on our sample. Hence, this approach can adequately capture the complex association between a modality of unstructured data and our outcome measures. However, its disadvantage is that it does not capture interactions between modalities via an end-to-end training approach, but instead only captures interactions by combining predicted values, and hence may lead to loss of information. We overcome this limitation with a multimodal approach in 5.3.

5.3 Multimodal Model

We show the architecture of our Multimodal model in Figure 4. It is based on Ghosal et al. (2018) and Wu et al. (2014), and has been adapted for our setting. We first obtain embeddings (using the same pre-trained models in 5.1) for text (captions/ transcript), audio and images (video frames) from each 30 second clip over the entire duration of each video (details in Online Appendix D.1). We pass embeddings for each clip from each modality as input to Bi-Directional GRU Layers that capture the sequential interdependence between each clip of a modality. This is followed up with a sequence of dense time-distributed layers and dense transformation layers that further process the data. In addition, we also obtain embeddings from the title, description (first 160c) and thumbnail of each video, which along with the structured features (listed earlier in Table 2), are supplied as input and processed through independent dense transformation layers. We then concatenate the output of the preceding seven layers and capture the interactions across modalities using a dense fusion layer (see Online Appendix D.1 for details).

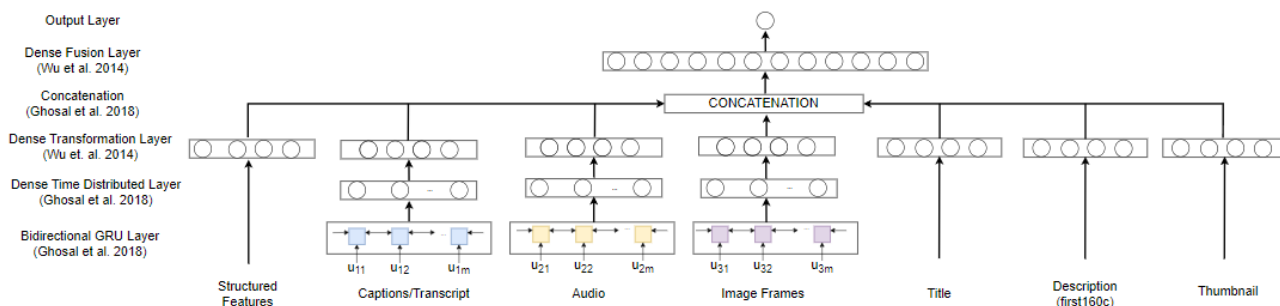


Figure 4: Multimodal Architecture

The advantage of this approach is that it trains the data end-to-end and hence captures interactions between latent dimensions of unstructured data during the training process. However, its disadvantage is that it leads to loss of information as we are training the model using embeddings of unstructured data and not the actual raw unstructured data. We are unable to simultaneously train raw unstructured data (along with structured features) with the benefit of transfer learning in an end-to-end approach due to the extremely high computational (and monetary) cost associated with such an undertaking which is typically accomplished by researchers at large corporations. Hence, we use both the approaches in 5.2 and 5.3 to

combine information from all modalities, as each approach has its distinct advantage.⁶Note that in the Multimodal Model, we first use the same data as that used in the Combined Model (30 seconds from the beginning, middle and end) in order to compare and contrast the findings of both approaches (results in 7.1.3). Subsequently, we validate whether the results of the Multimodal Model hold true when using data from the entire video (results in 8.1). Next, we explain our approach towards interpretation in Section 6.

6. Interpretation Approach

We detail the implementation of our interpretation approach discussed earlier in Section 3.2 and Figure 3. In 6.1, we detail Step 1 of our interpretation approach that uses the importance measures estimated from the individual models (discussed in 5.1). In 6.2, we discuss Step 2 of our interpretation approach that uses the outcome values predicted by the individual models. We describe our process to generate the theory-based features (discussed in 3.3) that we use as features of interest (in 6.1 & 6.2) in Online Appendix E.

6.1 Interpreting Relationship with Importance (Step 1)

After finding the estimated attention weights from the Text model for each word-piece in captions/transcript, we implement Step 1 of the interpretation approach 12 times by analyzing the following equation for each outcome (four outcomes) and each 30 second part⁷ of the video – beginning, middle and end (three parts):

$$\log(\text{AttentionWeight}_{itk}) = \alpha_i + \gamma X_{it} + \sum_{k=1}^{n_b} \beta_{1k}(\text{BIT}_{itk}) + \sum_{k=1}^{n_e} \beta_{2k}(\text{EIT}_{itk}) + \beta_3(\text{TP}_{itk}) + \beta_4(\text{NOT}_{it}) + \epsilon_{itk} \quad (2)$$

where, $\text{AttentionWeight}_{itk}$ is the estimated weight for each token k (word-piece created from raw text by the model) in video t made by influencer i , α_i is influencer fixed effects, X_{it} is the same vector of structured features used earlier in equation (1). BIT_{itk} is ‘brand indicator in token’ indicating whether token k is a brand name, EIT_{itk} is ‘emotion indicator in token’ indicating whether token k is an emotional word, TP_{itk} is token k ’s position in the text, NOT_{it} is number of tokens in the text, n_b is total number of brands, n_e is total number of emotional words, and ϵ_{itk} is the error. We use a unique coefficient for each brand and emotional word to model potential heterogeneity in effects. We use a covariate for the token position (TP_{itk}) to control for any potential influence of the position of the word-piece in the text, and we control for the number of tokens (NOT_{it}) because attention weights in text are relative to each other and sum up to one, i.e. more the number of tokens, lower will be the attention directed to it.

⁶ A multimodal model that trains *raw* unstructured data from various sources (followed with estimation of attention weights and gradients) is computationally infeasible in an academic/university setting as the estimation time is of the order of years. Note that a Multi-Task Learning (MTL) approach to simultaneously predict all four outcomes is not suitable here because one of our primary goals is to interpret the relationship between theory-based features and *each* engagement measure independently.

⁷ Note that we cannot simultaneously control for presence of features in all parts of the video in the same equation in Step 1 because the number of observations (e.g., tokens k) in each part of the video may be different (see Table 9 & 11 in Sec 7.2 for difference in number of observations).

After finding the estimated attention weights for each sound moment from the Audio model, we implement Step 1 of the interpretation approach 12 times by analyzing the following equation for each outcome (four outcomes) and each 30 second part of the video – beginning, middle and end (three parts):

$$\log(\text{AttentionWeight}_{itk}) = \alpha_i + \gamma X_{it} + \beta_1(CI(\text{Human})_{itk}) + \beta_2(CI(\text{Music})_{itk}) + \beta_3(CI(\text{Human})_{itk} \times CI(\text{Music})_{itk}) + \beta_4(CI(\text{Animal})_{itk}) + \beta_5(CI(\text{Other})_{itk}) + \beta_6(\text{Location}_{itk}) + \epsilon_{itk} \quad (3)$$

where, $\text{AttentionWeight}_{itk}$ is the estimated weight for moment k in video t made by influencer i , α_i is influencer fixed effects, X_{it} is the same vector of structured features used earlier in equation (1), $CI(\text{Human})$ is the Category Indicator for human sounds in moment k , and $CI(\text{Human}) \times CI(\text{Music})$ corresponds to moments when both human and music sounds occur together, Location_{itk} corresponds to location of the moment within 60 moments of the audio clip, and ϵ_{itk} is the error. We use a covariate for the location so that we can control for any potential influence of the position of the moment. Note that we do not include a covariate for number of audio moments, as each clip has the same length of 30 seconds.

After finding the estimated gradient values from the Image model, we implement Step 1 of the interpretation approach 12 times by analyzing the following equation for each outcome (four outcomes) and each 30 second part of the video – beginning, middle and end (three parts):

$$\text{MeanGradientValues}_{itk} = \alpha_i + \gamma X_{it} + \sum_{k=1}^8 \beta_{1k} \text{SizeObject}(k)_{it} + \beta_{21} \text{Joy}(\text{Face})_{itk} + \beta_{22} \text{Surprise}(\text{Face})_{it} + \beta_{23} \text{Joy}(\text{Face})_{it} \times \text{SizeObject}(\text{Face})_{it} + \beta_{24} \text{Surprise}(\text{Face})_{it} \times \text{SizeObject}(\text{Face})_{it} + \epsilon_{itk} \quad (4)$$

where, $\text{MeanGradientValues}_{itk}$ is the mean gradient values across the area (pixels) occupied by all items of object category k across 30 frames in video t made by influencer i , α_i is influencer fixed effects, X_{it} is the same vector of structured features used earlier in equation (1), and $k = 1$ to 8 corresponds to each object category: {humans, faces, animals, brand logos, packaged good, clothes & accessories, home & kitchen and other objects}. $\text{SizeObject}(k)_{it}$ is the mean across 30 frames of the percentage of the image occupied by all objects of category k in video t made by influencer i . Hence, the coefficient β_{1k} can be interpreted as the effect of a one percent increase in size of the object of category k on average across 30 seconds of the video. Note that features for size of humans and size of faces are not highly correlated (variance inflation factor ≤ 2.5 across each video part). $\text{Joy}(\text{Face})_{it}$ and $\text{Surprise}(\text{Face})_{it}$ indicate the mean (across 30 frames) of the level of surprise or joy in each face {-2: very unlikely, -1: unlikely, 0: possible, 1: likely, 2: very likely}. The two interaction terms capture the interaction between the emotion registered and the size of faces, and ϵ_{itk} is the error.

6.2 Interpreting Relationship with Outcome (Step 2)

After finding predicted outcome values from each of the Text, Audio and Image models, we implement Step 2 of the interpretation approach 36 times by analyzing the following equation for each outcome and each part of a video {3 models x 4 outcomes x 3 parts of video}:

$$\begin{aligned}
PredictedOutcome_{it} = & \alpha_i + \gamma X_{it} + \sum_{p \text{ in part}} \left\{ \sum_{k=1}^{n_b} \beta_{1pk} (BITX_{it}) + \sum_{k=1}^{n_e} \beta_{2pk} (EITX_{it}) + \beta_{3p} (NOT_{it}) + \right. \\
& \beta_{4p} (Sum \text{ of } CI(Human)_{it}) + \beta_{5p} (Sum \text{ of } CI(Music)_{it}) + \beta_{6p} (Sum \text{ of } CI(Human)_{it} \times Sum \text{ of } CI(Music)_{it}) + \\
& \beta_{7p} (Sum \text{ of } CI(Animal)_{it}) + \beta_{8p} (Sum \text{ of } CI(Other)_{it}) + \sum_{k=1}^8 \beta_{9pk} SizeObject(k)_{it} + \beta_{10p} Joy(Face)_{it} + \\
& \beta_{11p} Surprise(Face)_{it} + \beta_{12p} (Joy(Face)_{it} \times SizeObject(Face)_{it}) + \\
& \left. \beta_{13p} (Surprise(Face)_{it} \times SizeObject(Face)_{it}) \right\} + \epsilon_{it} \tag{5}
\end{aligned}$$

where, $PredictedOutcome_{it}$ is a predicted outcome from a model for a part of video t made by influencer i , α_i is influencer fixed effects and X_{it} is the same vector of structured features used earlier in equation (1). $BITX_{it}$ is a ‘brand indicator in text’ indicating whether the text (captions/transcript) in video t by influencer i has a brand, $EITX_{it}$ is ‘emotion indicator in text’ indicating whether the text has an emotional word, and NOT_{it} is number of tokens in the text. As done in equation (2), we use a unique coefficient for each brand and emotional word to model potential heterogeneity in effects. We control for the number of tokens (NOT_{it}) to control for the potential influence of the length of the text on the outcome variable. $Sum \text{ of } CI(Human)_{it}$ corresponds to the duration of human sounds (or sum of the Category Indicator for human sounds) across the 30 seconds (60 moments) in video t made by influencer i , and $Sum \text{ of } CI(Human)_{it} \times CI(Music)_{it}$ finds the total duration when human and music sounds occur together. As we have controlled for the number of tokens (word-pieces), an increase in $Sum \text{ of } CI(Human)_{it}$ can be interpreted as slower speech whereas a decrease in $Sum \text{ of } CI(Human)_{it}$ can be interpreted as rapid speech. The other variables are identical to those used in equation (4). In summary, we control for features across all sources of unstructured data (that were used earlier in the three equations of Step 1). We also sum over the $parts = \{\text{beginning, middle, end}\}$ of the video in equation (5) to control for the presence of words, sounds and objects in different locations of the video.

The values of the coefficients corresponding to each feature across Step 1 (Eq 2, 3 or 4) and Step 2 (Eq 5) will inform us whether the feature has a strong correlation with the predicted outcome (Step 2) that is also supported by an increase in importance attributed to the feature (Step 1).

7. Results

In this section, we discuss the results of prediction in 7.1 and interpretation in 7.2.

7.1 Prediction Results

We divide our random sample of 1620 videos into a random 60% training sample (972 videos), 20% validation sample (324 videos) and 20% holdout sample (324 videos). We present results using data from the beginning, middle and end 30 seconds for all videos in our sample (as discussed in Section 5.1).

7.1.1 Individual Models

We train the model on the training sample, tune the number of steps of Adam gradient descent on the validation sample, and then compute predictive performance on the holdout sample. Our parameter

choices during model training are guided by the standard values used in the BERT, YAMNet and VGG-16 models. Importantly, we implement a form of bootstrapping, by repeating model training, validation and prediction 50 times (25 times) for every covariate-outcome pair in the Text and Audio models (Image Model) to mitigate concerns of model brittleness.⁸ This can be an issue if our models converge to different (local) optima in every instance of model training due to sensitivity to starting values of *hyperparameter* weights randomly chosen by our deep learning models.

We compare the predictive performance of our models with other standard benchmark models used in the marketing literature to demonstrate that our interpretable models do not compromise on predictive ability. We show the detailed results of predictive performance in Online Appendix F, and summarize the key results here. We find that our Text model (BERT) has better prediction error than benchmarks such as LSTM, CNN (Liu et al., 2019), CNN-LSTM (Chakraborty et al., 2022) and CNN-Bi-LSTM. This demonstrates the benefit of a model that captures contextual word embeddings, has hierarchical layers and a self-attention mechanism. The Audio model has better prediction error than benchmarks that do not use transfer learning. This demonstrates that addition of transfer learning not only helps with interpretability but also contributes towards the predictive ability of the Audio model. The Image model (VGG-16) has better prediction error than a conventional 4-layer CNN on thumbnail images, thus demonstrating the benefit of transfer learning and a deeper architecture. Overall, we demonstrate that our interpretable models perform better than or at least as well as, other standard predictive models and thus we do not compromise on predictive ability (details in Online Appendix F). Table 5 summarizes the prediction errors from our models, for each component of unstructured data, and for each of the four outcome measures of engagement.

Our models predict all the continuous outcomes (commentability, thumbsability and likeability) with a RMSE ranging from 0.69 to 1.03 and the binary outcome (loveability) with accuracies ranging from 63% to 72%. For example, *captions/transcript in the beginning 30s* can be used to predict commentability within an average RMSE range of $\pm e^{0.92} = \pm 2.5 \frac{\#comments+1}{\#views}$. Importantly, the sample standard deviation for the error and accuracy values across all the bootstrap iterations range from 0.01 to 0.03 across all our covariate-outcome pairs. The low value of the standard deviation demonstrates that our model iterations are quite stable. Of all the sources of unstructured data, the title of the video has the best out-of-sample predictive performance, which suggests that *title* is able to better discriminate between engagement values of different influencers' videos and/or within same influencers' videos.

⁸ We carry out our analysis using one NVIDIA RTX A6000 GPU (48GB RAM) and 128GB CPU RAM, that takes the maximum time to analyze the Image model. For 25 bootstrap iterations, it takes around 36 hours to run the model and complete the gradient analysis for each covariate-outcome pair (e.g. beginning 30 sec-loveability). It takes a total of 432 hours {36 hours x 4 outcomes x 3 video parts} to analyze all pairs. Hence, for computational ease, we restrict the number of iterations to 25 for the Image model, but go up till 50 iterations for the Text and Audio models.

Model	Unstructured data	Deep Engagement		Shallow Engagement	
		Love-ability	Comment-ability	Like-ability	Thumbs-ability
Text Model (BERT)	Title	0.72	0.83	0.84	0.69
	Description (first 160c)	0.70	0.87	0.94	0.72
	Captions/transcript (begin 30s)	0.71	0.92	0.98	0.75
	Captions/transcript (middle 30s)	0.69	0.98	1.03	0.79
	Captions/transcript (end 30s)	0.67	0.98	1.03	0.78
Audio Model (YAMNet + Bi-LSTM + Attention)	Audio (begin 30s)	0.64	0.92	1.01	0.80
	Audio (middle 30s)	0.63	0.95	1.02	0.80
	Audio (end 30s)	0.65	0.96	1.01	0.79
Image Model (VGG-16)	Thumbnail	0.68	0.96	1.00	0.78
Image Model (VGG-16 + Bi-LSTM)	Video Frames (begin 30s @1fps)	0.66	0.92	0.99	0.77
	Video Frames (middle 30s @1fps)	0.66	0.96	0.99	0.77
	Video Frames (end 30s @1fps)	0.67	0.94	0.98	0.75

Table 5: Model performance for each component of unstructured data in holdout sample (RMSE for Commentability, Thumbsability and Likeability; Accuracy for Loveability)

We also find that the prediction error while using any of the unstructured components of captions/transcript, audio and video frames (in each part of the video) are close to each other while predicting all engagement measures. This demonstrates two important things. First, it shows that each of the three individual models (Text, Audio and Image) perform comparatively well (when using information from each part of the video) in capturing variation in engagement. Second, it suggests that information in text, audio and images within video content are highly correlated with each other.

7.1.2 Combined Model

To estimate the Combined Model in 5.2, we first re-predict each of our individual models in 5.1 on the entire sample (training, validation and holdout) to obtain \hat{Y}_{it} for video t by influencer i . We repeat this process for all bootstrap iterations and obtain the average of the predicted values. We then combine them with structured features X_{it} (as shown earlier in Eq (1)) using different combined models, g . We train each combined model on the training sample, validate the hyperparameters on the validation sample, and obtain predictions on the holdout sample (see results in Table 6).

	Commentability	Loveability	Thumbsability	Likeability
OLS	0.78	0.74	0.63	0.77
Ridge Regression	0.73	0.74	0.56	0.71
LASSO	1.17	0.73	0.96	1.29
Elastic Net	1.12	0.74	0.91	1.20
Deep Neural Net	0.77	0.74	0.56	0.73
Random Forests	0.73	0.74	0.59	0.76
XGBoost	0.77	0.72	0.63	0.76

Table 6: Performance of different Combined Models on holdout sample (RMSE for commentability, thumbsability and likeability; Accuracy for loveability)

We find that Ridge Regression, a linear model, has the best performance on the holdout sample for all continuous outcomes (lowest RMSE) and the binary outcome (highest accuracy) as compared to

OLS, LASSO, Elastic Net, Deep Neural Net, Random Forest and XGBoost (see Table 6). This suggests that structured features and the predictions from individual models for unstructured data do not have substantial interactions with each other.

Note that the predicted outcomes from the individual models (\hat{Y}_{it}) supplied as features to the Combined Model can be collinear with each other. However, all features with multicollinearity in the Ridge Regression model are regularized equally towards the null, and hence their relative importance can be captured by the model. We measure relative importance of each feature by taking the magnitude of each estimated coefficient from the Ridge Regression model applied on the training sample and scale it by the sum of the magnitude of all coefficient values. This gives us the relative importance (*marginal effect*) or percentage contribution of each feature while predicting each engagement measure.⁹ This is shown in Table 7 (Panel A). Note that as the features used in the model (\hat{Y} in Eq 1) can be collinear, the feature importance measures should be interpreted as conveying a combination of *between-influencer* (different influencers’ videos) and *within-influencer* (same influencer’s videos) importance of a feature.

			Deep Engagement		Shallow Engagement	
			Loveability	Comment-ability	Likeability	Thumbs-ability
Panel A	Structured Features	Influencer Fixed Effects	18.0%	2.9%	31.8%	39.5%
		Other features (Table 2)	36.8%	2.4%	7.7%	10.5%
		Total	54.8%	5.4%	39.4%	49.9%
	Unstructured data					
	Incentive to Click Data	Title	9.4%	25.4%	15.5%	9.9%
		Description (first 160c)	9.1%	22.7%	13.0%	7.6%
		Thumbnail	0.1%	2.6%	1.9%	2.2%
		Total	18.5%	50.8%	30.3%	19.7%
	Captions / Transcript	Begin 30s	5.7%	13.7%	9.5%	7.1%
		Middle 30s	5.7%	10.7%	4.7%	5.6%
		End 30s	5.7%	7.4%	4.4%	5.5%
		Total	17.0%	31.7%	18.7%	18.2%
	Audio	Begin 30s	1.1%	3.0%	1.0%	1.7%
		Middle 30s	0.8%	1.0%	1.2%	1.3%
		End 30s	0.7%	1.7%	1.7%	1.9%
		Total	2.6%	5.7%	3.8%	4.9%
	Video Frames	Begin 30s	4.1%	3.0%	2.4%	2.4%
		Middle 30s	1.0%	1.2%	2.0%	2.1%
		End 30s	2.0%	2.4%	3.3%	2.6%
		Total	7.1%	6.5%	7.7%	7.1%
Panel B	Total Begin 30s		10.9%	19.7%	12.9%	11.2%
	Total Middle 30s		7.4%	12.8%	7.9%	9.1%
	Total End 30s		8.4%	11.4%	9.4%	10.0%

Table 7: Importance of features based on the Combined Model

⁹ As we scale all the features by their L^2 norm before running the model, the coefficients are regularized to the same degree and hence we can make relative comparisons. Also, we sum up the coefficient values that lie within a class (e.g., sum up coefficient values of influencer fixed effects, sum up other structured features (in Table 5)) to get an overall idea of the contribution of a class of features in predicting each outcome.

We find that influencer fixed effects are especially important for predicting measures of shallow engagement (39.5% for thumbsability and 31.8% for likeability). This suggests that characteristics unique to an influencer are more important in predicting automatic reactions from viewers. Now, “incentive to click” data (title, description – first 160c, thumbnail) are more likely to drive a change in views than engagement, since they are visible in search results and prompt the viewer to click on a video. However, their power in explaining engagement with the video suggests correlation between them and the content of the video. This is especially prominent for title and description (first 160 characters) which explain more variation in all the engagement measures than thumbnail images do.

Importantly, we find that captions/transcript explain more than *twice* the variation in all engagement measures than audio or video frames across each part of the video (beginning, middle or end). This suggests that words spoken by the influencer are more influential in capturing variation in engagement than audio-visual features. However, the difference in importance between audio and video frames is minimal. Overall, we can conclude that “what is said” (words spoken) is more important than “how it is said” (imagery or acoustics) to distinguish between engagement levels of different videos (by the same or different influencer). Note that these conclusions are possible because the Text, Image or Audio model predict comparatively well when using captions/transcript, video frames, or audio respectively (across each part of the video) as discussed earlier in 7.1.1. Hence the results inferred from Table 7 should not be attributed to better predictive ability of an individual model as compared to another, but to the stronger marginal impact of the modality of text (captured by captions/transcript data).¹⁰

These findings show that the substance of the message (in captions/transcript) conveyed by the influencer is more influential than the presentation choice in imagery (video frames) or acoustics (audio). This is consistent with the age-old advertising adage of Ogilvy – “*What you say is more important than how you say it: the information you give is more important to the consumer than the way you present it.*” (Ogilvy, 1983). Our finding is also novel to the broader advertising literature, as previous literature has not documented the relative influence of these three modalities (in ad videos) on marketing outcomes, to the best of our knowledge. While our findings are correlational, they provide general directions along which improvements are more likely. Hence, influencers may benefit from prioritizing working on their choice of words, followed by the choice of imagery or acoustics.

Next, we analyze the relative importance of unstructured data in each part of the video in Table 7 (Panel B). We find that, on average, unstructured data in the beginning of videos explain more variation in all the engagement measures than unstructured data in the middle or end of videos. This insight is informative as it provides evidence that viewers need not watch videos completely before making the

¹⁰ A closer examination reveals that the Text model has *significantly* better predictive ability than Audio or Image model in only 33% of the 12 occasions (4 outcomes x 3 parts of video) in Table 5. Despite that, in Table 7, text is always more important (has a stronger marginal impact) than audio or images across all 100% of the 12 occasions. Hence, the higher importance of text should be attributed to the data and not to the model.

decision to engage with it. This is also consistent with the fact that many viewers indeed do not finish watching YouTube videos (Bump, 2021). Thus, influencers may focus more energy on designing the beginning than later parts of videos to improve engagement.

7.1.3 Multimodal Model

We train the model on the training sample, tune the number of steps of Adam gradient descent on the validation sample, and then compute predictive performance on the holdout sample. Our parameter choices during model training are guided by the standard values used in the multimodal architecture of Ghosal et al. (2018). As done in 7.1.1, we repeat model training, validation and prediction 50 times and obtain the average of the prediction errors to mitigate concerns of model brittleness. We show the results in Table 8. We find that the prediction error from the Multimodal Model is a lot worse than the prediction error that was observed earlier using the Combined Model in Table 6. This demonstrates that the loss of information from using embeddings is a lot more than the advantage of capturing interactions between modalities via the training process. Hence, the Multimodal model is less suited for ex-post interpretation as compared to the individual models (used in the Combined Model) that capture richer information.

	Commentability	Loveability	Thumbsability	Likeability
Prediction Error	0.84	0.69	0.71	0.91
Permuted Prediction Error: Text (Captions/Transcript)	0.99	0.52	0.80	1.04
Permuted Prediction Error: Audio	0.88	0.69	0.73	0.94
Permuted Prediction Error: Image (Video Frames)	0.88	0.69	0.76	0.95
Difference in Permuted Prediction Error: Text vs Audio	0.10***	-0.16***	0.07***	0.10***
Difference in Permuted Prediction Error: Text vs Image	0.11***	-0.17***	0.04***	0.08***
Note: *** $p < 0.001$				

Table 8: Results of Multimodal Model (Embeddings from Begin, Middle and End 30s)
(RMSE for commentability, thumbsability and likeability; Accuracy for loveability)

In order to measure relative importance of the modalities (features), we use Permutation Feature Importance (PFI) which is defined as the magnitude of the worsening in prediction error (*increase in RMSE and decrease in accuracy*) when a feature is randomly permuted between observations (Fisher et al., 2019; Molnar et al., 2021). For example, to test whether text (captions/transcript) is important, the embeddings of text are permuted between observations in the holdout sample, but the remaining features are held constant. The magnitude of the worsening in prediction error will inform us about the strength of association (or magnitude of the marginal effect) between text (captions/transcript) and the outcome that was captured during the training process. This is similar to the way feature importance is measured in random forests.¹¹ In addition, we use the following approach to find the relative importance of modalities:

¹¹ Note that we do not use the more conventional leave-one-feature-out approach to measure feature importance as that is not suitable when features are highly collinear as is the case in our setting between text, audio and images (discussed in 7.1.1). This is because if one feature is left-out during model training and prediction is carried out on the holdout sample, then the effect of the missing feature on the outcome will be compensated by the other collinear features. The leave-one-feature-out approach assigns more importance to features that are unique and not

if modality A is more important than modality B, then the worsening in prediction error from permuting modality A will be more than the worsening in error from permuting modality B. This approach is also consistent with the way we measured feature importance in 7.1.2 where we captured relative marginal effects of features in the Combined Model.

First, we focus on finding the relative importance between text (captions/transcript), audio and images (video frames). We compare the difference in prediction errors between the permuted modalities across the 50 bootstrap iterations using a t-test and show the difference in means in Table 8. We find that text is significantly more important than audio or images (*as there is an increase in RMSE or decrease in accuracy*) while predicting each of our engagement measures, consistent with the findings for the Combined Model in Table 7. This demonstrates that even when we account for interactions between modalities during the training process, text remains more important than audio or images. Note that the difference in means between audio and images is minimal (consistent with results of the Combined Model), suggesting that these modalities have comparable importance. Second, we also find that the beginning 30 seconds (across text, audio and images) is significantly more important than the middle or end, also consistent with results of the Combined Model in Table 7 (see details in Online Appendix D.2).

We validate whether the superiority of text over audio or images also holds true when using information from the entire video (and not just the beginning, middle and end 30 seconds) in Section 8.

7.2 Interpretation Results

We use the individual deep learning models for ex-post interpretation. We do so by re-predicting each of our individual models on the entire sample of 1620 videos to take advantage of complete information in our data. Note that our interpretation is carried out for each bootstrap iteration that is repeated 50 times (25 times) for every covariate-outcome pair in Text and Audio models (Image Model), to mitigate potential concerns of brittleness (as discussed earlier in 7.1).

7.2.1 Interpretation Results for Text Model

We estimate equation (2) (Step 1) using Ridge Regression to capture heterogeneity in effects across brands and emotional words. Similarly, we estimate equation (5) (Step 2) using Ridge Regression (and present additional reasons for our modelling choice in Online Appendix G.1). In order to obtain the ridge parameter, we train equation (2) on the training sample over a wide array of ridge parameters, then validate it on the validation sample to obtain the ridge parameter that minimizes loss. We then use this ridge parameter and estimate equation (2) over the entire sample of videos.

necessarily to features that are more informative (which have a strong marginal effect) (Fisher et al., 2019). We use the measure of the magnitude of the marginal effect of a feature (and not the amount of unique information in a feature) as a measure of feature importance.

We present the results of the analysis for brand and emotion mentions in Table 9. The table displays the percentage of total brands and percentage of total emotional words whose median coefficient value (across 50 bootstrap iterations) has a positive effect (+) on predicted attention weights (Eq 2) and a positive (+) and/or negative effect (-) on predicted outcome (Eq 5). However, when calculating this percentage, we ignore brands/emotions whose value is less than 5% of the magnitude of the maximum predictive effect on the respective outcome in Eq (2) or (5). We use this *bar* of 5% (robustness discussed ahead) so that we can ignore non-important predictors whose coefficients have been shrunk towards 0 by the Ridge Regression model. We highlight in grey the cells that represent the dominant directional effect of brands/emotions on predicted outcome. For these cells, we also show (in the row below) the average across all brands/emotional words of the average frequency (over 50 bootstrap iterations) with which a brand/emotional word (that meets the 5% bar) continues to have a positive effect on attention weight and the dominant directional effect on predicted outcome. We highlight those cells in green where the effect on attention weight (Step 1) and predicted outcome (Step 2) is in the same direction (+/-) at least 80% of the time. Our choice of the 80% threshold (as compared to a less conservative 50% even chance threshold) lends more confidence that these results are less likely to be spurious. Similarly, we highlight those cells in orange where the effect is in the same direction in only one of Step 1 or Step 2 at least 80% of the time, and these cells are more likely to represent spurious relationships.

			Sentiment of Engagement			
			Brands		Emotions	
			Deep	Shallow	Deep	Shallow
			Loveability	Likeability	Loveability	Likeability
	(Eq 2) Attention Weights (AW) (Step 1)	(Eq 5) Predicted Outcome (PO) (Step 2)				
Beginning	+	+	21.6%	38.6%	8.3%	29.0%
	% of time AW +, PO +			76%, 92%		77%, 90%
	+	-	42.5%	29.4%	23.3%	19.5%
	% of time AW +, PO -		85%, 93%		79.5%, 93%	
Middle	+	+	20.0%	26.4%	11.4%	22.1%
	% of time AW +, PO +			77%, 86%		76%, 86%
	+	-	36.4%	21.8%	20.3%	16.5%
	% of time AW +, PO -		82%, 93%		78%, 95%	
End	+	+	18.4%	33.3%	9.4%	20.3%
	% of time AW +, PO +			76%, 86%		77%, 87%
	+	-	40.2%	26.4%	20.5%	16.9%
	% of time AW +, PO -		79%, 94%		79%, 94%	
Sample Size: N = 114,536 tokens in beginning 30s, 107,411 tokens in middle 30s, 83,607 tokens in end 30s (Step 1); N = 1620 videos (Step 2) Bar: 5% (% of max coefficient value used to ignore non-important predictors that have been shrunk towards 0 by Ridge Regression) Highlighted grey cells: Dominant directional effect of brands/emotions on predicted outcome. Highlighted green (<i>orange</i>) cells: Average across all brands/emotions of the average frequency with which a brand/emotion has the same directional effect is at least 80% across 50 iterations in both (<i>only one of</i>) Step 1 and Step 2.						

Table 9: Interpretation results of the Text model

We find that a majority of brand mentions in the beginning or middle of the video are more often assigned high importance (Step 1) and more often have a negative association with predicted loveability

(deep engagement) (Step 2). We also show a graphical visualization of these key results in Online Appendix G.2. We also carry out a robustness check to ensure that (for the results highlighted in green) the association holds true across a range of values of the *bar* used in Table 9 (details in Online Appendix G.2). In other words, we demonstrate how our findings are robust to brand mentions that have a small or a large negative association with loveability. Also, as per theory, we do not expect any association between use of brands or emotional words and measures of commentability and thumbsability. Our results also do not show evidence of a robust association.

Our findings for brand mentions suggest that a decrease in entertainment value resulting from a discussion of commercial content in the beginning or middle may activate the deliberate System II thinking in the minds of more viewers in turn making them respond unfavorably or neutrally to the video in their comments, thus decreasing loveability (Teixeira et al., 2010; Tellis et al., 2019). This is consistent with prior research that has found a decrease in sharing of commercial content on YouTube (Tellis et al., 2019). Hence, we find more compelling evidence for one of the competing hypotheses discussed earlier in 3.3.1. Notably, the negative association with loveability is dominated by brands in the electronics and digital categories, and related ads can be more informative and less entertaining as associated products are typically more functional and less hedonic. This is consistent with the theoretical mechanism of a reduction in entertainment value which could be driving the effect. We do not find compelling evidence of a relationship between emotional words and sentiment of shallow or deep engagement.

Overall, we identify two relationships (green cells) at the intersection of Step 1 & 2 that are less likely to be spurious, and exclude 10 relationships (orange cells) from Step 2 which are more likely to be spurious. Note that we do not find likely spurious relationships in Step 1 that lie above the 80% threshold.

7.2.2 Interpretation Results for Audio Model

We estimate equations (3) (Step 1) and (5) (Step 2) using OLS (for continuous outcomes) and logistic regression (for binary outcome) on the entire sample of videos (see details in Online Appendix G.3). The results are shown in Table 10. The table shows the median value of estimated coefficients, $\hat{\beta}$, across 50 bootstrap iterations, where the coefficient value reflects a percent change in the (non-log-transformed) outcome when a sound moment is present (Eq 3) or sound duration increases by one moment (Eq 5). The rows below each coefficient reflect the percentage of time (across 50 iterations) the corresponding p value is statistically significant. Similar to our approach in 7.2.1, we highlight those cells in green (orange) that are significant at least 80% of the time in both (only one of) Step 1 and 2.

We summarize a few of the key results corresponding to the cells in green. As can be seen in Table 10, an increase in duration of music (without simultaneous speech) by one moment (about half a second) within the beginning 30 seconds is associated with an increase in the odds ratio of loveability by 30.6% (Eq 5), but also a decrease in commentability by 2.0% (Eq 5). These associations are significant

100% of the time across our 50 iterations (Eq 5) and are also supported by a significant increase in attention at least 90% of the time (Eq 3). These effects are especially dominant in the beginning than in the middle or end of the video, as evidenced by the more frequent positive significant effects for attention (>90%) in the beginning (Eq 3) when the feature is new and more salient. However, the association between music in the first 30 seconds and measures of shallow engagement is weaker or significant less often, suggesting that music has a stronger association with measures of deep than shallow engagement.

The positive association between the duration of music and the sentiment of deep engagement is consistent with our general expectation in 3.3.2 where we discussed the positive affective influence of music in advertising literature (Pelsmacker & Van den Bergh, 1999). In addition, our finding of a reduction in commentability suggests that there may also be a net reduction in the number of negative comments below the video, which could contribute to the increase in loveability. Overall, the strong association between music in the beginning and our measures of deep engagement suggests that music strongly influences deliberate reactions from viewers (System II thinking).

		Deep Engagement						Shallow Engagement					
		Loveability			Commentability			Likeability			Thumbsability		
		Begin	Middle	End	Begin	Middle	End	Begin	Middle	End	Begin	Middle	End
Eq (3) Attention Weights (Step 1)	Human β_1	-3.9%	17.8%	-0.4%	2.6%	9.5%	0.0%	0.0%	24.7%	1.0%	0.0%	2.5%	9.4%
	p <= 0.05	49%	55%	58%	60%	86%	50%	56%	82%	50%	52%	78%	68%
	Music β_2	248.3%	78.8%	-0.6%	13.9%	4.7%	0.0%	0.0%	15.9%	0.1%	0.5%	3.3%	1.3%
	p <= 0.05	96%	63%	52%	92%	54%	74%	82%	60%	80%	82%	56%	64%
	H x M β_3	-54.4%	-46.0%	3.9%	-5.3%	-7.1%	0.0%	0.0%	-5.8%	0.0%	0.0%	-1.1%	0.0%
	p <= 0.05	90%	65%	64%	78%	82%	62%	68%	60%	72%	60%	58%	42%
	Animal β_4	354.3%	1325.2%	111.7%	0.0%	0.0%	0.0%	0.0%	52.5%	0.0%	0.0%	1.1%	10.1%
p <= 0.05	90%	80%	92%	46%	20%	78%	52%	68%	72%	38%	44%	68%	
Eq (5) Predicted Outcome (Step 2)	Human β_1	-2.5%	-6.5%	-4.6%	-0.2%	0.1%	-0.4%	0.2%	0.3%	0.3%	-0.1%	-0.1%	-0.4%
	p <= 0.05	29%	69%	46%	38%	48%	82%	78%	90%	74%	40%	52%	90%
	Music β_2	30.6%	20.5%	16.4%	-2.0%	-1.4%	-1.5%	-0.3%	0.0%	-0.2%	-0.9%	-0.7%	-1.1%
	p <= 0.05	100%	96%	96%	100%	100%	100%	78%	50%	70%	100%	100%	100%
	H x M β_3	-18.0%	-7.6%	-15.1%	-0.4%	0.2%	0.7%	0.1%	0.1%	0.0%	-0.1%	0.1%	0.4%
	p <= 0.05	82%	61%	64%	52%	52%	82%	58%	54%	24%	34%	66%	54%
	Animal β_4	51.5%	72.6%	98.0%	-0.1%	0.6%	1.6%	0.8%	1.2%	1.2%	-0.5%	0.7%	4.3%
p <= 0.05	59%	57%	84%	2%	38%	82%	90%	96%	76%	20%	74%	94%	

Sample Size: N = 97,200 moments in beginning 30s, middle 30s or end 30s (Step 1); N= 1620 videos (Step 2)
 Highlighted green (orange) cells: p value is significant ≤ 0.05 at least 80% of the time across 50 iterations in both (only one of) Step 1 and Step 2 and coefficient in Step 1 is positive (because negative attention weight indicates non-important coefficient).

Table 10: Interpretation results of the Audio Model

We also find no occasion where the coefficient for the duration of human sounds is *negative* in Step 2 and significant more than 80% of the time in both steps. This suggests that there is no strong association between *rapid* speech in any part of the video and our measures of engagement, consistent with the expectation of linguists who have analyzed influencer videos (Beck, 2015; Jennings, 2021). Note that a decrease in the duration of human sounds can be interpreted as rapid speech because we control for the number of word-pieces, as discussed earlier in Section 6.2. However, we do observe a positive

association between *slower* speech (*positive* coefficient for duration of human sounds) in the middle 30 seconds and likeability, suggesting that the middle of the video maybe an important place to slow down.

Overall, as shown in Table 10, we exclude relationships corresponding to orange cells that are more likely to be spurious. This corresponds to 4 relationships (corresponding to Eq 3) that are only frequently significant in Step 1, and 14 relationships (corresponding to Eq 5) that are only frequently significant in Step 2. By using a two-step process we identify a smaller subset of 5 relationships (green cells) at the intersection of Step 1 and Step 2 that are less likely to be spurious.

7.2.3 Interpretation Results for Image Model

We estimate equations (4) and (5) using OLS (for continuous outcomes) and logistic regression (for binary outcome) on the entire video sample (see details in Online Appendix G.3). The results are shown in Table 11. The table shows the median value of estimated coefficients, $\hat{\beta}$, across 25 bootstrap iterations, where the coefficient value reflects a percent change in the (non-log-transformed) outcome when size of an object increases by one percent on average across 30 video frames. The rows below each coefficient reflect the percentage of time (across 25 iterations) the corresponding p value is statistically significant. As done in 7.2.2, we highlight those cells in green (orange) that are significant at least 80% of the time across both (only one of) Step 1 and 2.

		Deep Engagement						Shallow Engagement					
		Loveability			Commentability			Likeability			Thumbsability		
		Begin	Middle	End	Begin	Middle	End	Begin	Middle	End	Begin	Middle	End
Eq (4) Mean Gradients (Step 1)	Humans $\hat{\beta}_{11}$	0.0%	0.0%	0.1%	0.8%	0.8%	0.9%	0.8%	0.8%	0.9%	0.9%	0.8%	0.9%
	p <= 0.05	100%	100%	96%	100%	100%	100%	100%	100%	100%	100%	100%	100%
	Faces $\hat{\beta}_{12}$	-0.2%	-0.1%	-0.2%	0.8%	0.5%	0.3%	0.6%	0.4%	0.3%	1.0%	0.6%	0.2%
	p <= 0.05	56%	12%	60%	100%	96%	56%	100%	100%	60%	100%	100%	48%
	Animals $\hat{\beta}_{13}$	0.2%	0.3%	0.3%	1.1%	1.1%	1.2%	1.2%	1.3%	1.4%	1.2%	1.2%	1.3%
	p <= 0.05	100%	100%	100%	100%	100%	100%	100%	100%	100%	100%	100%	100%
	B Logos $\hat{\beta}_{14}$	0.0%	-0.1%	0.0%	0.1%	-0.2%	0.2%	-0.1%	-0.2%	0.0%	0.0%	-0.1%	0.1%
	p <= 0.05	0%	0%	0%	0%	0%	0%	0%	0%	0%	0%	0%	0%
	P Goods $\hat{\beta}_{15}$	0.1%	-0.1%	0.0%	0.7%	0.7%	0.8%	0.7%	0.7%	0.6%	0.7%	0.5%	0.7%
p <= 0.05	0%	0%	0%	100%	96%	100%	100%	100%	100%	96%	100%	92%	96%
Eq (5) Predicted Outcome (Step 2)	Humans $\hat{\beta}_{11}$	0.0%	1.5%	1.8%	0.3%	0.2%	0.0%	0.4%	0.2%	0.4%	0.4%	0.3%	0.1%
	p <= 0.05	8%	76%	60%	64%	52%	44%	92%	96%	92%	96%	96%	48%
	Faces $\hat{\beta}_{12}$	7.4%	3.4%	3.3%	0.9%	0.0%	0.6%	0.4%	0.5%	-0.8%	0.9%	0.9%	0.4%
	p <= 0.05	48%	16%	12%	44%	48%	24%	0%	52%	32%	68%	96%	28%
	Animals $\hat{\beta}_{13}$	5.3%	4.1%	13.3%	0.6%	0.0%	0.0%	1.0%	0.6%	1.7%	0.9%	0.4%	0.6%
	p <= 0.05	16%	4%	100%	56%	16%	36%	100%	88%	100%	96%	36%	88%
	B Logos $\hat{\beta}_{14}$	8.6%	22.8%	1.6%	-0.6%	0.0%	0.8%	0.4%	-0.4%	-3.8%	0.3%	-1.2%	0.1%
	p <= 0.05	8%	8%	0%	0%	0%	4%	0%	0%	72%	0%	12%	4%
	P Goods $\hat{\beta}_{15}$	-1.6%	-3.1%	-3.6%	-0.2%	0.0%	0.0%	-0.7%	0.0%	-0.3%	-0.5%	-0.2%	0.2%
p <= 0.05	8%	0%	8%	4%	28%	24%	88%	8%	12%	84%	0%	12%	

Sample Size: N = 5868 objects in beginning 30s, 5659 objects in middle 30s and 5519 objects in end 30s (Step 1); N = 1620 videos (Step 2)
Highlighted green (orange) cells: p value is significant ≤ 0.05 at least 80% of the time across 25 iterations in both (only one of) Step 1 and Step 2

Table 11: Interpretation results of the Image Model

We summarize a few of the key results corresponding to the cells in green. An increase in size of human images by 1% in the beginning, middle or end of a video is associated with a 0.4%, 0.2% or 0.4% increase in likeability (sentiment of shallow engagement) respectively which is consistent with our expectations in 3.3.3. These associations are significant at least 90% of the time across our 25 iterations (Eq 5) and are also supported by a significant increase in attention 100% of the time (Eq 3). However, we do not find a corresponding positive association with the sentiment of deep engagement that is frequently significant across both Steps 1 and 2. This demonstrates that human images elicit automatic and intuitive reactions from viewers that can manifest easily as a like for the video. Furthermore, the association between size of face and sentiment of shallow or deep engagement is not frequently significant. This demonstrates that the image of the entire human is more important, when controlling for the size of the face. This is reasonable because the size of the whole human will be correlated with the area of the screen where they are demonstrating something to the viewer with the help of their hands.

We also find evidence that an increase in size of packaged goods by 1% in the beginning 30 seconds is associated with a decrease in likeability (sentiment of shallow engagement) by 0.7%. Overall, both the previous findings for human images and packaged goods are consistent with Hartmann et al. (2021) who find that consumer selfies (i.e., human images) receive more likes than brand selfies and packshots (i.e., packaged goods) on Instagram. The desire to socialize, engage and communicate with other humans is likely driving these effects (Hartmann et al., 2021; To & Patrick, 2021; Xiao & Ding, 2014). Notably, our results are true for sentiment of shallow engagement but not sentiment of deep engagement suggesting that the desire for social interaction is manifested more easily in quick reactions.

We also find that an increase in size of animals by 1% in the beginning, middle or end of video is associated with a 1.0%, 0.6% or 1.7% increase in likeability respectively. This is consistent with our expectation as ads featuring animals have been found to be more likeable and have an extremely low irritation score (Biel & Bridgwater, 1990; Pelsmacker & Van den Bergh, 1999). We do not find frequent significant associations between facial expressions of joy or surprise and our measures of engagement which is consistent with results found in related domains (Li & Xie, 2020; Zhou et al., 2021). It is important to note that inferences of emotion (made either by humans or API's) on facial expressions in images rely on commonly based heuristics and need not reflect the true emotion being experienced by the person (Barrett et al., 2019). This could be one of the main reasons for not observing significant effects. We also do not find frequent significant associations for everyday objects such as clothes & accessories and home & kitchen items. Hence, we do not report their coefficient values in Table 11. Overall, we identify 14 relationships (green cells) at the intersection of Step 1 and Step 2, and exclude 25 relationships (orange cells corresponding to Eq 4) that are more likely to be spurious and only frequently significant in Step 1. Note that we do not find likely spurious relationships in Step 2 that lie above the 80% threshold.

7.2.4 Summarizing Insights

We used a two-step process for identifying a subset of relationships between features of interest in text, audio or images and engagement. We filtered out likely spurious relationships from Steps 1 and 2, and identified relationships at the intersection. The majority of these relationships correspond to the beginning 30 seconds of the video, which demonstrates that features in the beginning are on average more salient and are also sufficient to prompt a viewer to engage with a video (consistent with our prediction-based findings in 7.1). We summarize these results for the beginning 30 seconds in Table 12.

Unstructured Data	Features	Deep Engagement		Shallow Engagement		Expected change in sentiment (Table 1)
		Love-ability	Comment-ability	Like-ability	Thumbs-ability	
Text: Captions/ Transcript	Brand names	–				Ambiguous
Audio	Music	+	–		–	Positive
Images: Video Frames	Human			+	+	Positive
	Animal			+	+	Positive
	Packaged goods			–	–	Negative

Table 12: Summary of key interpretation results for the beginning 30 seconds

We show the direction of association between a feature and an outcome by a + or – sign. These relationships are obtained while controlling for features across all sources of unstructured and structured data. Hence, they are unlikely to be confounded with observed features in our data. However, our approach does not guarantee causality of the identified relationships. Hence, using theory (discussed earlier in Section 3.3), we validate many of the identified relationships at the intersection (cells highlighted in grey). Importantly, we find distinct associations with respect to measures of shallow or deep engagement, a difference that has not been pinpointed in prior research. For the beginning 30 seconds, we find that our *features in text and audio* have an association with *sentiment of deep engagement*, whereas our *features in images* have an association with *sentiment of shallow engagement*. Moreover, we are also able to resolve the ambiguity with respect to the association between brand mentions and sentiment (discussed earlier in Section 3.3.1). Overall, our two-step approach prunes spurious associations, thus significantly reducing the effort required for future causal testing.

8. Validation

We conduct systematic analyses to validate the approach (and results) for prediction and interpretation.

8.1 Validating Prediction Approach

We validate whether the main results of the prediction approach hold true using data from the complete video and not just the beginning, middle and end 30 seconds. We accomplish this efficiently using the multimodal approach shown earlier in Figure 4, where we create embeddings from each successive 30-second clip of a video. For videos shorter than the longest video in our sample, we add padded

embeddings with constant values corresponding to empty segments, so that all videos have the same number of time-steps. We pass embeddings from each time step (30-second clip) as input to the Bi-Directional GRU layers (in 7.1.3 we did it for three time steps - beginning, middle and end). We show the results in Table 13 for the difference in permuted prediction error at different video durations analyzed.

We find that for video durations up to 18.5 min (90th percentile of duration in our sample), text is significantly more important than audio or images for all outcomes. However, for longer durations we observe some non-significant effects which is primarily an artifact of the large variance in duration across our sample.¹² Overall, text continues to be significantly more important than audio or images in predicting engagement even when we use information from the entire video and not just the beginning, middle or end. Note that the difference in means between audio and images is minimal and hence the effect is not always significant (similar to our findings in 7.1.2 & 7.1.3), and hence we do not report those values.

Maximum duration of video analyzed (A)	Corresponding video percentile duration (B)	No. of 30 sec time steps	Modality Comparison	Commentability	Loveability	Thumbsability	Likeability
5.5 min	50% [#]	11	Text vs Audio	0.12***	-0.13***	0.09***	0.14***
			Text vs Images	0.15***	-0.13***	0.09***	0.14***
18.5 min	90% [#]	37	Text vs Audio	0.06***	-0.01**	0.02***	0.02***
			Text vs Images	0.06***	-0.01**	0.02***	0.02***
25 min	95% [#]	50	Text vs Audio	0.04***	-0.01 ^{n.s.}	0.01***	0.01***
			Text vs Images	0.04***	-0.01 ^{n.s.}	0.01***	0.01***
271.6 min	100% ^{##}	544	Text vs Audio	0.00001 ^{n.s.}	0 ^{n.s.}	0.00002**	0.00001*
			Text vs Images	0.00003***	0 ^{n.s.}	0.00003***	0.00001**

[#]Embeddings from full duration of B% of videos. Remaining (100-B) % of videos are truncated at A min.
^{##}Embeddings from full duration of 100% of videos. Significance codes: ***p<0.001, **p<0.01, *p<0.05, ^p<0.1, n.s. p ≥ 0.1 (not significant).

Table 13: Difference in Permuted Prediction Error: Results of Multimodal Model (Embeddings from whole video) (RMSE for commentability, thumbsability and likeability; Accuracy for loveability)

8.2 Validating Interpretation Approach

We validate our interpretation approach in three ways. First, we carry out simulations to demonstrate that our ex-post interpretation approach is able to recover the true data generating process while also removing spurious relationships across both Step 1 and Step 2. Second, we apply benchmark feature selection methods to the simulated data to demonstrate how our results are different and better. Finally, we carry out ex-post interpretation by estimating equation (5) on a random 80% sample of the 1620 videos, and find that all the substantive findings summarized earlier in Table 12 continue to hold true with approximately the same effect sizes and frequency of significance as before. This demonstrates that our

¹² For video durations longer than 18.5 min, padded embeddings become a lot more dominant as they occupy a large majority of the time-steps. Hence, when observations are permuted to measure relative feature importance, the overall design of the matrix of covariates does not change enough (because values of padded embeddings remain constant). This results in a decrease in the magnitude of the ‘difference in permuted prediction error’ and hence we observe a few non-significant effects.

main results are not sensitive to the size of our chosen sample, and that our transfer learning methods work effectively with moderate sized samples, increasing the feasibility and efficiency of analysis. Next, we elaborate on the simulation procedure and comparison with benchmarks.

We simulate an outcome to vary based on specific features in either text, audio or images. We then carry out model training as done in Section 7.1 using the covariates from our data. We follow this up with ex-post interpretation as done in Section 7.2. We also apply the following benchmark feature selection approaches – LASSO and Elastic Net (0.5L1,0.5L2) – to our simulated data, as these methods have been known to reliably select important predictors in other contexts. Specifically, we test whether these benchmark methods can recover the data generating process in our setting without going through the two-step process. We apply these methods to capture the relationship between the features in our data and the predicted outcome returned by the deep learning models. Note that we implement bootstrap iterations 50 (25) times for the Text and Audio models (Image model) across all approaches.

8.2.1 Text Model – Simulation and Benchmarks

To simulate the outcome for the Text Model, we pick a covariate-outcome pair, say “brand mentions in beginning 30 seconds of captions/transcript – likeability”. We generate a random normal distribution of log-likeability such that the mean and standard deviation across the observations where a brand is present is twice the mean and half the standard deviation of the observations where a brand is absent (details in Online Appendix H). We show the results of ex-post interpretation in Table 14 (analogous to Table 9).

We find that brands that meet the 5% *bar* (same as that in Table 9) are more often associated with an increase in predicted likeability (66.7% brands) than a decrease in predicted likeability (0.7% brands). Note that the % values corresponding to an *increase (decrease)* reflect the % of brands whose median coefficient value is *positive (negative)* and above the 5% bar across all bootstrap iterations. Furthermore, (the average across all brands of) the average frequency with which a brand (that meets the 5% bar) is associated with an increase in attention weights (Step 1) and predicted outcome (Step 2) is 91% and 97% respectively which is greater than the 80% threshold used by us in Section 7.2. The results are also robust to changes in the value of the *bar* (details in Online Appendix H). Thus, our interpretation approach using text data is able to recover the true data generating process associated with brand mentions. On the other hand, for emotion mentions, we find that they too are more often associated with an increase in predicted likeability (25.6% vs 21.5%). However, the average frequency with which emotion mentions are associated with an increase in attention weights and an increase in predicted likeability is 78% and 90% respectively, with the former being lower than the 80% threshold. Thus, our two-step approach is able to eliminate the spurious association between emotional words and predicted likeability.

Both the benchmark methods, LASSO and Elastic Net, also find that brands are more often associated with an increase (16.3% brands in LASSO and 19.6% brands in Elastic Net) than a decrease in

predicted likeability (0.7% brands in LASSO and 0.7% brands in Elastic Net) and are hence able to recover the true data generating process. However, both LASSO and Elastic Net also make the same conclusion regarding emotional words as they too are more often associated with an increase (5.7% emotional words in LASSO and 8% emotional words in Elastic Net) than a decrease in predicted likeability (1.8% emotional words in LASSO and 2% emotional words in Elastic Net). We also show in the table the average across all brands/emotional words of the average frequency (over 50 bootstrap iterations) with which a brand/emotional word continues to have a positive effect on predicted outcome (PO+). We find that that the percentage values are *higher* for emotional words (69% LASSO and 70% Elastic Net) than brands (67% LASSO and 69% Elastic Net) which is not consistent with the true data generating process since brands and not emotional words affect the simulated outcome. Hence, we are unable to reliably eliminate the spurious association with emotional words using the benchmark methods.

		Text Outcome: Likeability	
		Brands	Emotions
Two-Step Approach Bar: 5%	Step 1 AW+, Step 2 PO+	66.7%	25.6%
	% of time AW +, PO +	91%, 97%	78%, 90%
	Step 1 AW+, Step 2 PO-	0.7%	21.5%
LASSO	PO+	16.3%	5.7%
	% of time PO+	67%	69%
	PO-	0.7%	1.8%
Elastic Net (0.5L1,0.5L2)	PO+	19.6%	8.0%
	% of time PO+	69%	70%
	PO-	0.7%	2.0%

AW: Attention Weight; PO: Predicted Outcome; Bar: 5% (% of max coefficient value used to ignore non-important predictors that have been shrunk towards 0 by Ridge Regression); Highlighted feature name in grey: True data generating process; Highlighted green (*orange*) cells: Average across all brands/emotions of the average frequency with which a brand/emotion has the same directional effect is at least 80% across 50 iterations in both (*only one of*) Step 1 and Step 2.

Table 14: Simulation and Benchmarks – Text model

8.2.1 Audio and Image Model – Simulation and Benchmarks

To simulate the outcome for the Audio model, we pick a covariate-outcome pair, say “music duration in beginning 30 sec – commentability.” We then generate a random normal distribution of log-commentability whose value *decreases* by 0.5 for a unit increase in music duration (details in Online Appendix H). We show the results of ex-post interpretation with median values of estimated coefficients across 50 bootstrap iterations in Table 15 (analogous to Tables 9 & 10). We find that the median value of the estimated coefficient for music duration in Step 2 is -0.47 which is approximately equal to the true value of -0.5 . The estimated value is significant 100% of the time in Step 2 (across all 50 iterations) and is also supported by significance 92% of the time in Step 1. We are also able to remove a spurious association with duration of animal sounds which is frequently significant in Step 2, but is not frequently assigned a positive attention weight in Step 1. Thus, we demonstrate that our interpretation approach using audio data is able to recover the true data generating process and eliminate spurious associations.

To simulate the outcome for the Image model, we pick a covariate-outcome pair of interest, say “size of human images in beginning 30 sec – likeability.” We then generate a random normal distribution of log-likeability whose value *increases* by 0.25 units for a unit increase in the mean size of human images across the first 30 frames of a video (details in Online Appendix H). In Table 15, we show the results of interpretation with median values of estimated coefficients across 25 iterations. We find that the median value of the estimated coefficient for size of human images in Step 2 is 0.13 which is close to the true value of 0.25. The estimated value is significant 100% of the time in Step 2 and is also supported by significance 100% of the time in Step 1. Our estimation process also shortlists two more spurious associations corresponding to size of animals and size of clothes & accessories (highlighted green). However, we are able to remove seven spurious associations that are significant more than 80% of the time in Step 1 but not Step 2 (highlighted orange). Thus, we are able to demonstrate that our interpretation approach using image data is able to shortlist the feature corresponding to the true data generating process (and recover a closeness to the true coefficient value) while removing many spurious associations.

		Two-Step Approach		LASSO	Elastic Net (0.5L1, 0.5L2)
		Step 1	Step 2		
	Feature	Sign of coefficient, % of time $p \leq 0.05$	Coefficient, % of time $p \leq 0.05$	Coefficient	Coefficient
Audio Outcome: Comment- ability	Human	- , 74%	0.016, 58%	0	0
	Music	+, 92%	-0.47, 100%	-198.82	-2.95
	Human x Music	- , 84%	-0.03, 54%	0	-0.25
	Animal	- , 72%	-0.13, 84%	0	0
Image Outcome: Likeability	Human	+, 100%	0.13, 100%	0	1.7
	Face	+, 100%	0.09, 64%	0	1.71
	Animal	+, 100%	0.05, 88%	0	0
	Brand Logo	- , 0%	-0.003, 0%	0	0
	Packaged Goods	+, 100%	0.02, 4%	0	0
	Clothes & Acc	+, 100%	0.04, 96%	0	1.11
	Home & Kitchen	+, 100%	0.005, 8%	0	0
	Other Objects	+, 100%	0.006, 4%	0	0
	Joy	- , 4%	-0.24, 8%	0	-0.39
	Surprise	- , 100%	-0.60, 72%	0	-0.78
	Joy x Face	- , 84%	0.01, 0%	0	-1.31
Surprise x Face	+, 100%	-0.02, 36%	0	-1.74	
Highlighted feature name in grey: True data generating process; Highlighted green (orange) cells: p value is significant ≤ 0.05 at least 80% of the time across all bootstrap iterations in both (only one of) Step 1 and Step 2 and coefficient in Step 1 (for Audio Model) is positive (because negative attention weight indicates non-important coefficient).					

Table 15: Simulation and Benchmarks – Audio and Image model

We also show the median value of the estimated coefficients obtained from LASSO and Elastic Net for the Audio and Image model in Table 15. LASSO is able to recover the feature corresponding to the true data generating process in the Audio model, but the coefficient value is highly biased (-198.82). However, LASSO is unable to recover the feature corresponding to the true data generating process in the Image model. On the other hand, Elastic Net is able to recover the features corresponding to the true data

generating process in both the Audio and Image model, and the bias for the coefficient values are reduced but are not better than that obtained from our two-step approach. Moreover, Elastic Net also selects one other spurious feature in the Audio model, and six other spurious features in the Image model. Our two-step approach selects no spurious feature in the Audio model, and selects only two other spurious features in the Image model. Overall, our two-step approach selects fewer spurious features, and also recovers the true data generating process with a smaller bias as compared to benchmark feature selection approaches.

9. Conclusion

This paper adds to the small body of work on an important and growing marketing mechanism, influencer marketing. The main vehicle used in influencer marketing is influencer videos sponsored by brands. There is virtually no research on how the constituent features of these videos are related to measures of shallow engagement (System I) and deep engagement (System II) that both influencers and marketers care about. We take the first step at documenting these distinct relationships and contribute to the academic literature on social media engagement. We accomplish this using an “interpretable deep learning” framework, where we first capture the relative importance of modalities (text vs audio vs images) during prediction, and then implement ex-post interpretation on the same model that made good out-of-sample predictions. We accomplish interpretation using a novel two-step approach that eliminates several spurious relationships in each step and shortlists a subset of relationships for formal causal testing. Our approach is validated using simulation studies and comparison with benchmarks methods.

9.1 Managerial Implications

The findings from our research can be useful for practitioners in many ways. First, our prediction-based results demonstrate that influencers’ choice of words helps distinguish engagement values more than imagery or acoustics. This insight empowers influencers by providing them general directions along which to prioritize their efforts while designing videos. Changing their choice of words could be easier and more cost effective for influencers than changing imagery (e.g., shooting location and use of visual effects) or acoustics (e.g., microphone quality and background music). Second, as mentions of electronics and digital brands are more often associated with a decrease in loveability, brands in these categories may find it useful to investigate whether the influencers they partner with are sacrificing entertainment value for an increase in informativeness while discussing their brands. Similarly, packaged good brands maybe better off having their images displayed in the middle of the video than in the beginning where it is associated with a decrease in likeability. Finally, our approach allows us to create a scoring mechanism to rate a video on different modalities and produce visual illustrations to identify areas of improvement

(details in Online Appendix I). Hence, brands can use our approach and results to modify their brand integration strategy while still complying with the FTC guidelines discussed earlier in Section 4.

9.2 Limitations and Future Directions

Given that the paper represents early work on the analysis of unstructured data in influencer videos, it suffers from some limitations. First, as we have no access to sales data from influencer campaigns, we use proxy metrics that, while relevant to marketers, may not be perfectly correlated to business metrics. Second, as our sample includes only influencers who are top performers (on at least one major influencer platform) in their respective categories and use brand endorsements, our substantive findings may not generalize to those influencers who are not top performers (on at least one major platform) or who never receive such endorsements. Third, the uncovered relationships between video features and outcomes, while based on a two-step process that eliminates several spurious relationships, do not guarantee causality. While many of these relationships can be validated by theory, their causal effects need to be confirmed in further research, e.g., via field experiments. Fourth, while YouTube is one of the most important influencer marketing platforms for long-form videos, there may be systematic differences in how influencer videos work on other platforms or newly launched platform extensions such as YouTube Shorts for short-form videos. Finally, our findings may vary by type of video (e.g., product reviews, unboxing videos, etc.) or type of device (e.g., mobile, desktop and tablet) used to view a video, but our results only capture the average effect. We hope that future work can address these limitations.

Funding and Competing Interests

All authors certify that they have no affiliations with or involvement in any organization or entity with any financial interest or non-financial interest in the subject matter or materials discussed in this manuscript. The authors have no funding to report.

References

- Alexomanolaki, M., Loveday, C., & Kennett, C. (2007). Music and memory in advertising: Music as a device of implicit learning and recall. *Music, Sound, and the Moving Image*, 1(1), 51-72.
- Bahdanau, D., Cho, K., & Bengio, Y. (2014). Neural machine translation by jointly learning to align and translate. *arXiv preprint arXiv:1409.0473*.
- Bakir, V., & McStay, A. (2018). Fake news and the economy of emotions: Problems, causes, solutions. *Digital journalism*, 6(2), 154-175.
- Barrett, L. F., Adolphs, R., Marsella, S., Martinez, A. M., & Pollak, S. D. (2019). Emotional expressions reconsidered: Challenges to inferring emotion from human facial movements. *Psychological science in the public interest*, 20(1), 1-68.
- Beck, J. (2015). *The Linguistics of 'YouTube Voice'*. Retrieved December 7 from <https://www.theatlantic.com/technology/archive/2015/12/the-linguistics-of-youtube-voice/418962/>
- Berger, J., & Milkman, K. L. (2012). What makes online content viral? *Journal of Marketing Research*, 49(2), 192-205.

- Biel, A. L., & Bridgwater, C. A. (1990). Attributes of likable television commercials. *Journal of Advertising Research*, 30(3), 38-44.
- Brooks, A. (2020, January 24). *As influencers increasingly create video content, what does this mean for brands?* <https://marketingtechnews.net/news/2020/jan/24/influencers-increasingly-create-video-content-what-does-mean-brands/>
- Bump, P. (2021). *Why People Click Out of YouTube Videos [New Data]*. Retrieved April 12 from <https://blog.hubspot.com/marketing/why-people-click-out-of-youtube-videos>
- Burnap, A., Hauser, J. R., & Timoshenko, A. (2023). Product aesthetic design: A machine learning augmentation. *Marketing Science*.
- Chakraborty, I., Kim, M., & Sudhir, K. (2022). Attribute sentiment scoring with online text reviews: Accounting for language structure and missing attributes. *Journal of Marketing Research*, 59(3), 600-622.
- Chen, L., Yan, Y., & Smith, A. N. (2022). What drives digital engagement with sponsored videos? An investigation of video influencers' authenticity management strategies. *Journal of the Academy of Marketing Science*, 1-24.
- Chen, S., & Chaiken, S. (1999). The heuristic-systematic model in its broader context.
- Cheng, M. M., & Zhang, S. (2023). Reputation Burning: Analyzing the Impact of Brand Sponsorship on Social Influencers. *Working Paper, Available on SSRN: 4071188*.
- Cournoyer, B. (2014, March 19). *YouTube SEO Best Practices: Titles and Descriptions*. <https://www.brainshark.com/ideas-blog/2014/March/youtube-seo-best-practices-titles-descriptions>
- Covington, P., Adams, J., & Sargin, E. (2016). Deep neural networks for youtube recommendations. Proceedings of the 10th ACM conference on recommender systems,
- Devlin, J., Chang, M.-W., Lee, K., & Toutanova, K. (2018). Bert: Pre-training of deep bidirectional transformers for language understanding. *arXiv preprint arXiv:1810.04805*.
- Dew, R., Ansari, A., & Toubia, O. (2022). Letting logos speak: Leveraging multiview representation learning for data-driven branding and logo design. *Marketing Science*, 41(2), 401-425.
- Dixon, C., & Baig, H. (2019, March 7). *What is Youtube comment system sorting / ranking algorithm?* <https://stackoverflow.com/questions/27781751/what-is-youtube-comment-system-sorting-ranking-algorithm>
- Dwoskin, J. (2021). *There's A Big Difference Between Likes and Comments*. Retrieved June 5 from <https://www.stampede.social/there-s-a-big-difference-between-likes-and-comments>
- Dzyabura, D., El Kihal, S., Hauser, J. R., & Ibragimov, M. (2023). Leveraging the power of images in managing product return rates. *Marketing Science*.
- Fisher, A., Rudin, C., & Dominici, F. (2019). All Models are Wrong, but Many are Useful: Learning a Variable's Importance by Studying an Entire Class of Prediction Models Simultaneously. *J. Mach. Learn. Res.*, 20(177), 1-81.
- FTC. (2020). *Disclosures 101 for Social Media Influencers*. https://www.ftc.gov/system/files/documents/plain-language/1001a-influencer-guide-508_1.pdf
- Gemmeke, J. F., Ellis, D. P., Freedman, D., Jansen, A., Lawrence, W., Moore, R. C., Plakal, M., & Ritter, M. (2017). Audio set: An ontology and human-labeled dataset for audio events. 2017 IEEE International Conference on Acoustics, Speech and Signal Processing (ICASSP),
- Ghosal, D., Akhtar, M. S., Chauhan, D., Poria, S., Ekbal, A., & Bhattacharyya, P. (2018). Contextual inter-modal attention for multi-modal sentiment analysis. proceedings of the 2018 conference on empirical methods in natural language processing,
- Gogolan, D. (2022). *Engagement Rate for All Social Media Platforms*. Retrieved January 11 from <https://www.socialinsider.io/blog/engagement-rate/>
- Goh, K.-Y., Heng, C.-S., & Lin, Z. (2013). Social media brand community and consumer behavior: Quantifying the relative impact of user-and marketer-generated content. *Information systems research*, 24(1), 88-107.
- Gomez, R. (2021). *8 ways customers interact and engage with your brand on social*. Retrieved May 19 from <https://sproutsocial.com/insights/social-media-interaction/>
- Google. (2016). *Consumer Insights*. <https://www.thinkwithgoogle.com/consumer-insights/consumer-trends/top-reasons-viewers-watch-youtube/>
- Google. (2020). *Add tags to videos*. <https://support.google.com/youtube/answer/146402?hl=en>
- Guo, C., Cao, J., Zhang, X., Shu, K., & Yu, M. (2019). Exploiting emotions for fake news detection on social media. *arXiv preprint arXiv:1903.01728*.
- Guo, P. J., Kim, J., & Rubin, R. (2014). How video production affects student engagement: An empirical study of MOOC videos. Proceedings of the first ACM conference on Learning@ scale conference,

- Hartmann, J., Heitmann, M., Schamp, C., & Netzer, O. (2021). The power of brand selfies. *Journal of Marketing Research*, 58(6), 1159-1177.
- Hopf, M. (2020). *NLP With Google Cloud Natural Language API*. <https://www.toptal.com/machine-learning/google-nlp-tutorial>
- Huang, Y., & Morozov, I. (2022). Video Advertising by Twitch Influencers. Available at SSRN 4065064.
- Hughes, C., Swaminathan, V., & Brooks, G. (2019). Driving Brand Engagement Through Online Social Influencers: An Empirical Investigation of Sponsored Blogging Campaigns. *Journal of Marketing*.
- Hwang, S., Liu, X., & Srinivasan, K. (2022). Voice Analytics of Online Influencers. *Working Paper*, Available at SSRN 3773825.
- Influencer Marketing Hub. (2022). *The State of Influencer Marketing*. [https://influencermarketinghub.com/ebooks/Influencer Marketing Benchmark Report 2022.pdf](https://influencermarketinghub.com/ebooks/Influencer_Marketing_Benchmark_Report_2022.pdf)
- Jennings, R. (2021). *How should an influencer sound?* Retrieved July 13 from <https://www.vox.com/the-goods/2021/7/13/22570476/youtube-voice-tiktok-influencer-sound>
- Kahneman, D. (2003). Maps of bounded rationality: Psychology for behavioral economics. *American economic review*, 93(5), 1449-1475.
- Klear. (2019). *Influencer Marketing Rate Card*. <https://klear.com/KlearRateCard.pdf>
- Landsberg, N. (2021). *60 Powerful Video Marketing Statistics*. <https://influencermarketinghub.com/video-marketing-statistics/>
- Lanz, A., Goldenberg, J., Shapira, D., & Stahl, F. (2019). Climb or Jump: Status-Based Seeding in User-Generated Content Networks. *Journal of Marketing Research*, 56(3), 361-378.
- Lee, D., Hosanagar, K., & Nair, H. S. (2018). Advertising content and consumer engagement on social media: Evidence from Facebook. *Management Science*, 64(11), 5105-5131.
- Lee, D., Manzoor, E., & Cheng, Z. (2022). Focused Concept Miner (FCM): An Interpretable Deep Learning for Text Exploration. Available at SSRN: <https://ssrn.com/abstract=3304756>
- Leung, F. F., Gu, F. F., Li, Y., Zhang, J. Z., & Palmatier, R. W. (2022). EXPRESS: Influencer Marketing Effectiveness. *Journal of Marketing*, 00222429221102889.
- Li, X., Shi, M., & Wang, X. S. (2019). Video mining: Measuring visual information using automatic methods. *International Journal of Research in Marketing*, 36(2), 216-231.
- Li, Y., & Xie, Y. (2020). Is a picture worth a thousand words? An empirical study of image content and social media engagement. *Journal of Marketing Research*, 57(1), 1-19.
- Liu, L., Dzyabura, D., & Mizik, N. (2020). Visual listening in: Extracting brand image portrayed on social media. *Marketing Science*, 39(4), 669-686.
- Liu, X., Lee, D., & Srinivasan, K. (2019). Large-scale cross-category analysis of consumer review content on sales conversion leveraging deep learning. *Journal of Marketing Research*, 56(6), 918-943.
- Lu, S., Xiao, L., & Ding, M. (2016). A video-based automated recommender (VAR) system for garments. *Marketing Science*, 35(3), 484-510.
- Maheshwari, S. (2018, November 11). *Are You Ready for the Nanoinfluencers?* <https://www.nytimes.com/2018/11/11/business/media/nanoinfluencers-instagram-influencers.html>
- McClure, B. (2020). *How much do influencers charge per post?* <https://impact.com/partnerships/how-much-do-influencers-charge-per-post/>
- Mitchell, A. A. (1986). The effect of verbal and visual components of advertisements on brand attitudes and attitude toward the advertisement. *Journal of Consumer Research*, 13(1), 12-24.
- Molnar, C., Freiesleben, T., König, G., Casalicchio, G., Wright, M. N., & Bischl, B. (2021). Relating the partial dependence plot and permutation feature importance to the data generating process. *arXiv preprint arXiv:2109.01433*.
- O'Connor, C. (2017, September 26). *Forbes Top Influencers: Meet The 30 Social Media Stars Of Fashion, Parenting And Pets (Yes, Pets)*. <https://www.forbes.com/sites/clareoconnor/2017/09/26/forbes-top-influencers-fashion-pets-parenting/>
- Ogilvy, D. (1983). *Confessions of an advertising man*. Atheneum New York.
- Parsons, J. (2017, August 24). *How Long Until Watching a YouTube Video Counts as a View?* <https://growtraffic.com/blog/2017/08/youtube-video-counts-view>
- Pei, A., & Mayzlin, D. (2022). Influencing social media influencers through affiliation. *Marketing Science*, 41(3), 593-615.
- Pelsmacker, P. D., & Van den Bergh, J. (1999). Advertising content and irritation: a study of 226 TV commercials. *Journal of international consumer marketing*, 10(4), 5-27.

- Peterson, R. A., Cannito, M. P., & Brown, S. P. (1995). An exploratory investigation of voice characteristics and selling effectiveness. *Journal of Personal Selling & Sales Management*, 15(1), 1-15.
- Petty, R. E., & Cacioppo, J. T. (1986). The elaboration likelihood model of persuasion. In *Communication and persuasion* (pp. 1-24). Springer.
- Pieters, R., & Wedel, M. (2004). Attention capture and transfer in advertising: Brand, pictorial, and text-size effects. *Journal of Marketing*, 68(2), 36-50.
- Pilakal, M., & Ellis, D. (2020). *YAMNet*. <https://github.com/tensorflow/models/tree/master/research/audioset/yamnet>
- Rishika, R., Kumar, A., Janakiraman, R., & Bezawada, R. (2013). The effect of customers' social media participation on customer visit frequency and profitability: an empirical investigation. *Information systems research*, 24(1), 108-127.
- Selvaraju, R. R., Cogswell, M., Das, A., Vedantam, R., Parikh, D., & Batra, D. (2017). Grad-cam: Visual explanations from deep networks via gradient-based localization. Proceedings of the IEEE international conference on computer vision,
- Social Media Week. (2017). *Social Media Metrics Compared: Which Are The Most Valuable?* Retrieved October 19 from <https://socialmediaweek.org/blog/2017/10/social-media-metrics-compared-valuable/>
- Statista. (2023). *Global Influencer Marketing Size from 2020 to 2025*. <https://www.statista.com/statistics/1328195/global-influencer-market-value/>
- Teixeira, T., Wedel, M., & Pieters, R. (2010). Moment-to-moment optimal branding in TV commercials: Preventing avoidance by pulsing. *Marketing Science*, 29(5), 783-804.
- Teixeira, T., Wedel, M., & Pieters, R. (2012). Emotion-induced engagement in internet video advertisements. *Journal of Marketing Research*, 49(2), 144-159.
- Tellis, G. J., MacInnis, D. J., Tirunillai, S., & Zhang, Y. (2019). What drives virality (sharing) of online digital content? The critical role of information, emotion, and brand prominence. *Journal of Marketing*, 83(4), 1-20.
- Tian, Z., Dew, R., & Iyengar, R. (2023). EXPRESS: Mega or Micro? Influencer Selection Using Follower Elasticity. *Journal of Marketing Research*, 00222437231210267.
- Timoshenko, A., & Hauser, J. R. (2019). Identifying customer needs from user-generated content. *Marketing Science*, 38(1), 1-20.
- To, R. N., & Patrick, V. M. (2021). How the eyes connect to the heart: The influence of eye gaze direction on advertising effectiveness. *Journal of Consumer Research*, 48(1), 123-146.
- Vashishth, S., Upadhyay, S., Tomar, G. S., & Faruqui, M. (2019). Attention interpretability across nlp tasks. *arXiv preprint arXiv:1909.11218*.
- Wilbur, K. C. (2016). Advertising content and television advertising avoidance. *Journal of Media Economics*, 29(2), 51-72.
- Woltman Elpers, J. L., Wedel, M., & Pieters, R. G. (2003). Why Do Consumers Stop Viewing Television Commercials? Two Experiments on the Influence of Moment-to-Moment Entertainment and Information Value. *Journal of Marketing Research (JMR)*, 40(4).
- Wu, Z., Jiang, Y.-G., Wang, J., Pu, J., & Xue, X. (2014). Exploring inter-feature and inter-class relationships with deep neural networks for video classification. Proceedings of the 22nd ACM international conference on Multimedia,
- Xiao, L., & Ding, M. (2014). Just the faces: Exploring the effects of facial features in print advertising. *Marketing Science*, 33(3), 338-352.
- Yang, J., Zhang, J., & Zhang, Y. (2023). Engagement that Sells: Influencer Video Advertising on TikTok. *Available at SSRN 3815124*.
- YouTube. (2020). *What is fair use?* <https://www.youtube.com/intl/en-GB/howyoutubeworks/policies/copyright/>
- Yue-Hei Ng, J., Hausknecht, M., Vijayanarasimhan, S., Vinyals, O., Monga, R., & Toderici, G. (2015). Beyond short snippets: Deep networks for video classification. *Proceedings of the IEEE conference on computer vision and pattern recognition*, 4694-4702.
- Zhang, M., & Luo, L. (2022). Can consumer-posted photos serve as a leading indicator of restaurant survival? Evidence from yelp. *Management Science*.
- Zhang, S., Lee, D., Singh, P. V., & Srinivasan, K. (2021). What makes a good image? Airbnb demand analytics leveraging interpretable image features. *Management Science*.
- Zhao, K., Hu, Y., Hong, Y., & Westland, J. C. (2020). Understanding Characteristics of Popular Streamers on Live Streaming Platforms: Evidence from Twitch.tv. *Available at SSRN 3388949*.
- Zhou, M., Chen, G. H., Ferreira, P., & Smith, M. D. (2021). Consumer Behavior in the Online Classroom: Using Video Analytics and Machine Learning to Understand the Consumption of Video Courseware. *Journal of Marketing Research*, 58(6), 1079-1100.

Online Appendices

Influencer Videos: Unboxing the Mystique

Online Appendix A – Operationalization of Text Model

We provide an overview of the implementation of our Text Model - the BERT Framework (Devlin et al., 2018) in A.1, and explain the architecture of the encoders and attention mechanism (used in the BERT framework) in A.2 and A.3 respectively.

A.1 BERT Framework

The BERT model converts a sentence into word-piece tokens¹ as done by state-of-the-art machine translation models (Wu et al., 2016). Furthermore, the beginning of each sentence is appended by the ‘CLS’ (classification) token and the end of each sentence is appended by the ‘SEP’ (separation token). For example, the sentence ‘Good Morning! I am a YouTuber.’ will be converted into the (word-pieces or) tokens [‘[CLS]’, ‘good’, ‘morning’, ‘!’, ‘i’, ‘am’, ‘a’, ‘youtube’, ‘##r’, ‘.’, ‘[SEP]’]. A 768-dimensional initial embedding learnt for each token during the pre-training phase is passed as input to the model, and is represented by the vector x_m in Figure A1, where m is the number of tokens in the longest sentence. This vector x_m has pre-learned contextual embeddings that will aid the model in capturing relationships with our four outcome variables.

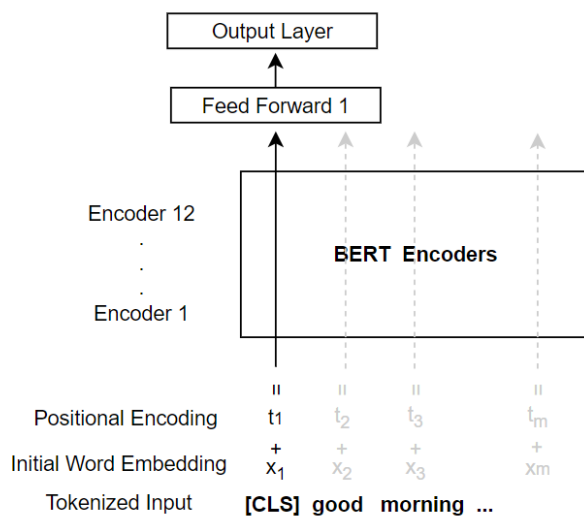


Figure A1: BERT Framework

The token embedding is combined with a positional encoder t_m that codes the position of the token in the sentence using sine and cosine functions (see Devlin et al. (2018) for details). This is passed through a set of 12 encoders arranged sequentially. The output of the ‘CLS’ token is passed through the

¹ We use the BERT-base-uncased model (that converts all words to lower case and removes accent markers) as compared to the cased model, because the uncased model is known to typically perform better unless the goal is to study case specific contexts such as ‘named entity recognition’ and ‘part-of-speech tagging.’

feed forward 1 layer that is initialized with pre-trained weights from the next sentence prediction task, and has a \tanh activation function. We follow this up with an output layer that connects with either of our three continuous outcomes or binary outcome. We then fine-tune the entire model with all hierarchical layers over our data sample.

The Encoders (explained in A.2) contain the self-attention heads (explained in A.3) which help the model capture the relative importance between word-pieces while forming an association with the outcome of interest. By virtue of being pre-trained to capture contextual usage of words, the model is able to make better decisions on assigning relative attention (importance) weights to different word-pieces (tokens) in our sample. Word-pieces that receive more attention play a more important role (in either a positive or negative direction) in predicting the outcome of interest. We analyze these attention weights during ex-post interpretation.

A.2 BERT Encoders

BERT Encoders comprise a set of 12 sequentially arranged identical encoders, and we illustrate the architecture of one encoder in Figure A2.²

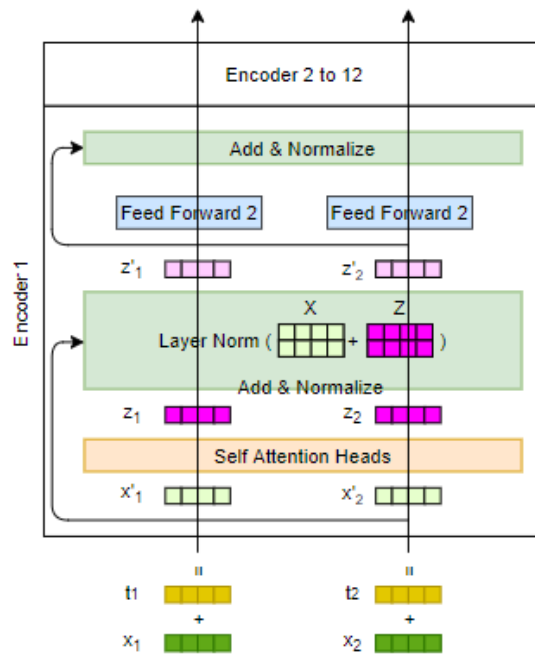


Figure A2: Encoders

We explain an example with a sentence that has only two tokens, and this can be extended to any example that has a maximum of 512 tokens, which is the maximum limit of the pre-trained BERT model.

² Our figures are inspired by the work of Jay Alammar (see Alammar (2018) for more details).

The combined vector of the initial token embedding (x_1, x_2) and positional encoding (t_1, t_2) results in the vectors (x'_1, x'_2) that are passed through self-attention heads which incorporate information of other relevant tokens into the focal tokens. The architecture of the self-attention head is explained in A.3. The outputs of the self-attention head (z_1, z_2) are then added with the original input (x'_1, x'_2) using a residual connection (shown with a curved arrow) and normalized (using mean and variance). The outputs (z'_1, z'_2) are passed through identical feed forward networks that have a GELU (Gaussian Error Linear Unit) activation function, i.e. $gelu(x) = 0.5x \left(1 + erf \left(\frac{x}{\sqrt{2}} \right) \right)$. The gelu activation combines the advantages of the ReLU (Rectified Linear Unit) non-linearity (i.e., $relu(x) = max(0, x)$) with dropout regularization. The outputs of the feed forward network are added with the inputs (z'_1, z'_2) using a residual connection and normalized again before being fed to the next encoder in sequence. In addition, each sub-layer is first followed by a dropout probability of 0.1 before being added and normalized.

A.3 BERT Attention Mechanism: Self-Attention heads

Next, we explain the self-attention heads that are illustrated in Figure A3. There are 12 self-attention heads that capture the contextual information of each token in relation to all other tokens used in the text. In other words, this allows the model to identify and weigh all other tokens in the text that are important when learning the vector representation of the focal token. We use this to measure the importance (strength) of association between the tokens in the text and the outcome of interest.

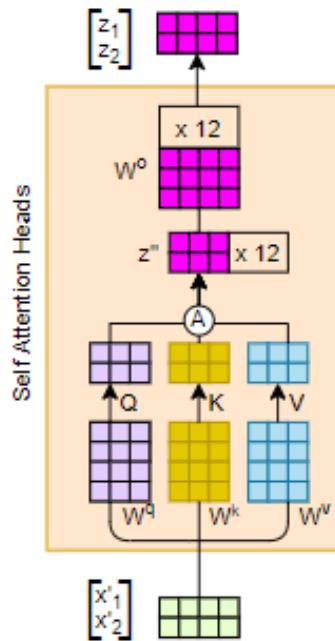


Figure A3: Self-Attention Heads

The inputs (x'_1, x'_2) are concatenated and multiplied with three weight matrices, W^q, W^k and W^v (that are fine-tuned during model training) to get three vectors – Q (Query), K (Key) and V (Value). These three vectors are combined using an attention function (A):

$$A(Q, K, V) = z''_0 = \text{softmax}\left(\frac{Q \cdot K^T}{\sqrt{d_k}}\right) \cdot V$$

where, d_k , the dimension of the Key vector, is 64 and is equal to the dimensions of the other two vectors d_q and d_v ; and $\text{softmax}(x) = \frac{e^{x_i}}{\sum_{i=1}^m e^{x_i}}$. The division by $\sqrt{d_k}$ is performed to ensure stable gradients. The computation of z''_0 is for one attention head, and this is carried out in parallel for 11 additional attention heads to give us 12 vectors, $z''_0 \dots z''_{12}$, which are concatenated to produce z'' . This is multiplied with a weight vector W^o (which is fine-tuned during model training) to produce output (z_1, z_2) . The use of 11 additional attention heads allows the model to capture more complex contextual information.

In order to capture the estimated attention weights, we average the output across all the attention heads in the last encoder of the BERT model, which results in an attention vector of dimension $\langle n, k, k \rangle$ where n is the number of videos used in the analysis, and $\langle k, k \rangle$ corresponds to k weights for k tokens, where k equals the maximum number of tokens (word-pieces) for a covariate type – title, description (first 160 characters) or captions/transcript (beginning, middle or end). As mentioned in A.1, the first token for each example is the ‘CLS’ or classification token. We are interested in the attention weights corresponding to this token because the output from this token goes to the output layer (as shown earlier in Figure A1). Thus, we get at an attention weight vector of dimension $\langle n, k \rangle$, where each observation has k weights corresponding to the ‘CLS’ token. We exclude ‘CLS’, ‘SEP’ and any token used for padding short sentences), during ex-post interpretation.

Online Appendix B – Operationalization of Audio Model

We provide an overview of the implementation of our Audio Model – YAMNet +Bi-LSTM+ Attention Mechanism in B.1, and explain the architecture of MobileNet v1 in B.2 and Bi-LSTM with attention mechanism in B.3.

B.1 YAMNet +Bi-LSTM+Attention Mechanism

We analyze audio data using the pre-trained YAMNet model (Pilakal & Ellis, 2020), and customize it with an additional Bidirectional LSTM (Bi-LSTM) layer and an attention mechanism as shown in the framework in Figure B1.

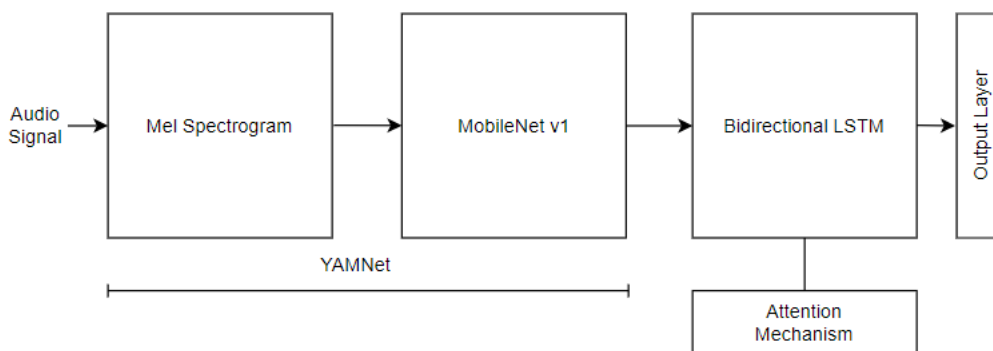


Figure B1: Audio Model Framework

Each audio signal is a 30 second clip, which we resample at 16,000 Hz and mono sound (for consistency), and this results in 480,000 data points for each clip. Note that for a few influencer videos that are shorter than 30 seconds, we append it with moments of silence to make the audio length consistent across our sample. To summarize the large number of data points, the YAMNet model first generates a Mel spectrogram that spans the frequency range of 125 to 7500Hz (note that the 2000-5000 Hz range is most sensitive to human hearing (Widex, 2016)) over which the YAMNet model has been pre-trained. The spectrogram uses the pre-trained Short-Term Fourier Transform window length of 25ms with a hop size of 10ms that results in a 2998 x 64 (time steps x frequency) vector corresponding to 30 seconds of each audio clip. This corresponds to 64 equally spaced Mel bins on the log scale, such that sounds of equal distance on the scale also sound equally spaced to the human ear. The model then passes each segment of 960ms from the spectrogram output, i.e., 96 frames of 10ms each with overlapping patches (to avoid losing information at the edges of each patch) as input to the MobileNet v1 architecture. The size of the overlap or hop size is 490ms, which results in a total of 60 moments for each 30 second audio clip.

The MobileNet v1 (explained in B.1) processes the spectrogram through multiple mobile convolutions and returns audio class predictions for each of the 60 moments in the clip. This comprise a

total of 521 different audio classes such as speech, music, animal, etc. (corresponding to each 960 ms segment) over which the model has been pre-trained. Pilakal and Ellis (2020) remove 6 audio classes (viz. gendered versions of *speech* and *singing*; *battle cry*; and *funny music*) from the original set of 527 audio classes to avoid potentially offensive mislabeling.

We then pass the $\langle 521 \times 60 \rangle$ dimensional vector as input to the Bi-Directional LSTM layer with an attention mechanism. We make this layer bidirectional to allow it to capture the interdependence between sequential audio moments from both directions. For example, the interdependence between the sound of a musical instrument at 5 seconds and the beginning of human speech at 15 seconds can be captured by the model bidirectionally. We adapt the attention mechanism used for neural machine translation by Bahdanau et al. (2014) (explained in B.3) to help the Bi-LSTM model capture the relative importance between sound moments in order to form an association with an outcome. These measures of relative importance (attention) can be understood similarly as the attention weights in the Text model, and are analyzed during ex-post interpretation. We pass the output of the Bi-LSTM (with attention mechanism) through an output layer which connects with either of our three continuous outcomes or binary outcome. We then fine-tune the Bi-LSTM with attention mechanism over our data sample.

B.2 MobileNet v1 architecture

The MobileNet v1 architecture is illustrated in detail in Table B1 (Howard et al., 2017). Each row describes Stage i with input dimension $[\hat{H}_i, \hat{W}_i]$ (resolution), output channels \hat{C}_i and \hat{L}_i layers (depth).

Stage i	Operator \hat{F}_i	Input Resolution $(\hat{H}_i \times \hat{W}_i)$	Output Channels \hat{C}_i	Depth \hat{L}_i (Layers)	Pre-trained Weights
1	Conv, k3x3, s2	96 x 64	32	1	Yes
2	MConv, k3x3, s1	48 x 32	64	1	
3	MConv, k3x3, s2	48 x 32	64	1	
4	MConv, k3x3, s1	24 x 16	128	1	
5	MConv, k3x3, s2	24 x 16	128	1	
6	MConv, k3x3, s1	12 x 8	256	1	
7	MConv, k3x3, s2	12 x 8	256	1	
8	MConv, k3x3, s1	6 x 4	512	5	
9	MConv, k3x3, s2	6 x 4	512	1	
10	MConv, k3x3, s2	3 x 2	1024	1	
11	Global Average Pooling	3 x 2	1024	1	
12	Dense	1 x 1	521	1	

Table B1: MobileNet-v1 architecture

Stage 1 has a regular convolution operation, whereas Stage 2 to 10 have the Mobile Convolution which is the main building block of the architecture. It is represented as “MConv, $k \times k$, s” where $k \times k = 3 \times 3$ is

the size of the kernel and $s = \{1,2\}$ is the stride. MConv divides the regular convolution operation into two steps – depth wise separable convolutions and point wise convolution, thus increasing the speed of computation (see Howard et al. (2017) for details). Stage 11 has a Global Average Pooling Layer that averages the inputs along its height and width and passes its output to Stage 12 which is a Dense output layer with 521 logistic functions that give the per class probability score corresponding to the 960 ms input segment. As mentioned earlier, we use a hop size of 490 ms so that we get an even number of 60 time step predictions corresponding to the 30 seconds of input. The resulting output vector has a dimension of 521x60 (audio classes x time steps) for each 30 second clip.

B.3 Bi-LSTM with Attention

The output from MobileNet v1 is passed as input to the Bi-LSTM with attention mechanism, shown in Figure B2.

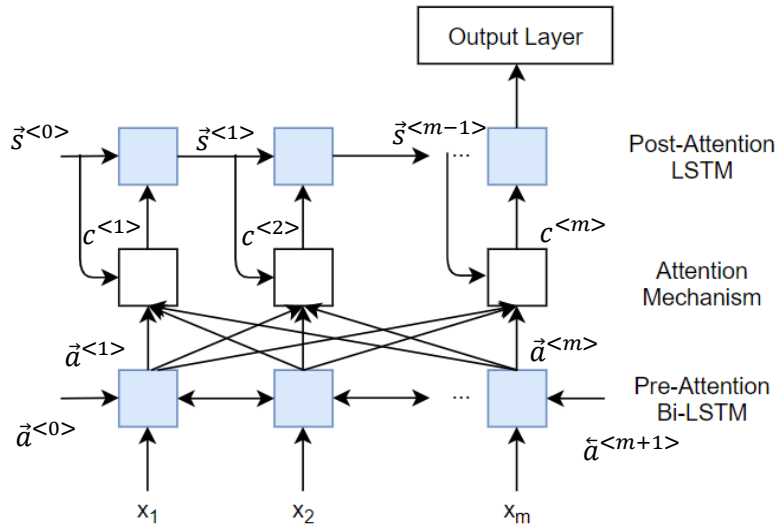


Figure B2: Bi-LSTM with Attention

We use two layers of LSTM cells – the first layer is a 32-unit Bidirectional LSTM layer and the second layer is a 64-unit (unidirectional) LSTM layer. They are separated by an attention mechanism as shown in the figure. Each audio segment $x_m <521,1>$, where m is the total number of moments (time steps), is passed as input to each cell of the Bidirectional LSTM layer. This layer is made bidirectional to allow it to capture the interdependence between sequential audio segments from both directions. The sequential nature of LSTM cells in a layer allow the model to capture dependencies between audio segments that are separated from each other (see the LSTM paper by Gers et al. (1999) for more details). We adopt the attention mechanism used for neural machine translation by Bahdanau et al. (2014) to help the Bi-LSTM model focus on more important parts of the input. The mechanism weighs the output activations ($a^{<t>} = [\vec{a}^{<t>}, \tilde{a}^{<t>}]$, $t = 1$ to m) from each cell of the pre-attention Bi-LSTM layer before

passing the contextual output, $c^{<t>}$, to the post-attention LSTM layer above it. In addition, each cell of the attention mechanism takes as input the output activation $s(t - 1)$ from each preceding cell of the post-attention LSTM layer which allows it to factor in the cumulative information learnt by the model till that time step (see Bahdanau et al. (2014) for more details on the attention mechanism). The output of the last cell in the post-attention LSTM layer is passed to an output layer which has a linear activation function for the three continuous outcomes and a sigmoid activation function for the binary outcome. The context vector $c^{<m>}$ from the last cell of the attention mechanism allows measurement of the relative weights placed by the model along the time dimension of the input in order to form an association with the outcome of interest. Audio moments that have higher weight are more important while forming an association between the audio clip and the outcome.

Online Appendix C – Operationalization of Image Model

We provide an overview of the implementation of our Image Model – VGG-16 +Bi-LSTM in C.1. We then explain the architecture of VGG-16 in C.2, the architecture to combine information from all video frames in C.3, and our approach to find gradient-based salient areas in C.4.

C.1 VGG-16 + Bi-LSTM

We use VGG-16 to analyze thumbnail images and a combination of VGG-16 and Bi-LSTM to analyze video frames. First, we pass thumbnail images as input to one VGG-16, and then finetune its final layers to capture relationship with each outcome. We provide details on the VGG-16 architecture in C.2. Next, we illustrate in Figure C1 our framework to analyze video frames. We pass each image frame $i = 1$ to m , where m has a maximum value of 30 frames, through a VGG-16 architecture. Our sampling rate of one frame per second (30 frames in 30 seconds) in conjunction with the size of our data sample (1620 videos) ensures that our model is feasible to analyze.

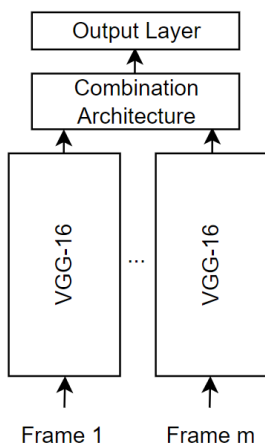


Figure C1: Framework to analyze Video Frames

In the last step, we combine the outputs from each VGG-16 model. Our combination architecture comprises the Bi-LSTM, known to be one of the best performing architectures at capturing sequential information from video frames (c.f. Yue-Hei Ng et al. (2015)). The output of the combination architecture is passed through an output layer which connects with either of our three continuous outcomes or binary outcome. We explain the combination architecture and fine-tuning process in more detail in C.3.

C.2 VGG-16 Architecture

VGG-16 has 16 layers whose parameters can be learned (Simonyan & Zisserman, 2014). The architecture of VGG-16, customized to our input dimension of $135 \times 240 \times 3$ (where 3 corresponds to pixel intensities for Red, Green and Blue channels), is shown in Table C1. Each row describes Stage i with input dimension $[\hat{H}_i, \hat{W}_i]$ (resolution), output channels \hat{C}_i and \hat{L}_i layers (depth).

Stage i	Operator \hat{F}_i	Input Resolution $(\hat{H}_i \times \hat{W}_i)$	Output Channels \hat{C}_i	Depth \hat{L}_i (Layers)	Pre-trained ImageNet weights
1	Conv, k3x3, s1	135 x 240	64	2	Yes
2	Max Pooling, k2x2, s2	135 x 240	64	1	
3	Conv, k3x3, s1	67 x 120	128	2	
4	Max Pooling, k2x2, s2	67 x 120	128	1	
5	Conv, k3x3, s1	33 x 60	256	3	
6	Max Pooling, k2x2, s2	33 x 60	256	1	
7	Conv, k3x3, s1	16 x 30	512	3	
8	Max Pooling, k2x2, s2	16 x 30	512	1	
9	Conv, k3x3, s1	8 x 15	512	3	
10	Max Pooling, k2x2, s2	8 x 15	512	1	
11	Global Average Pooling	4 x 7	512	1	No
12	Dense	1 x 1	1	1	

Table C1: VGG-16 architecture

Stages 1, 3, 5, 7 and 9 have convolution operations, whereas Stages 2, 4, 6, 8 and 10 have the max pooling operation, where $k \times k = 3 \times 3$ is the size of the kernel and $s = \{1,2\}$ is the stride. To analyze thumbnails, we use the pre-trained weights from Stage 1 to 10, and tune the weights of Stage 11 and 12. Stage 11 has a Global Average Pooling Layer that averages the inputs along its height and width and passes its output to Stage 12 which is a Dense output layer. The output layer has a linear activation function for the three continuous outcomes and a softmax activation function for the binary outcome.

C.3 Combination Architecture

To analyze video frames ($i = 1$ to m , where m has a maximum value of 30) we use the Bi-LSTM architecture that captures sequential information across different video frames. This is illustrated in Figure C2. Each VGG-16 architecture takes a unique video frame as input and provides the output from Stage 10 to the Global Average Pooling (GAP) Layer. This is followed by Dense Middle Layers (that use ReLU activation for continuous outcomes and sigmoid activation for the binary outcome), which is followed by a single Bi-LSTM layer with 256 memory cells, and finally a Dense output layer (that uses linear activation for continuous outcomes and softmax activation for the binary outcome). We use the pre-trained ImageNet weights (Krizhevsky et al., 2012) from Stage 1 to 10 in each VGG-16 architecture and then we finetune the weights of the top layers.

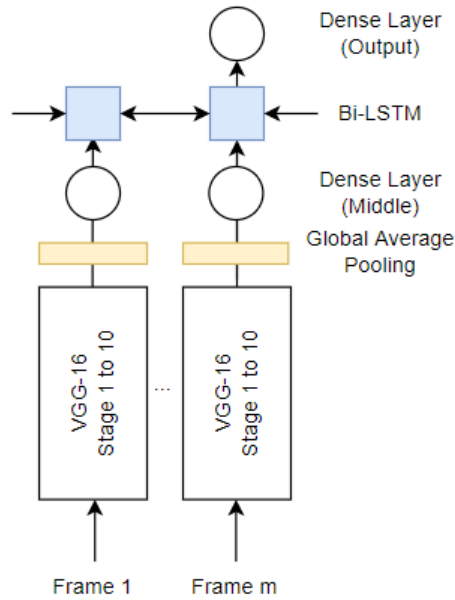


Figure C2: Bi-LSTM Combination

C.4 Gradient-based saliency

As our VGG-16 model uses pretrained weights from the ImageNet classification task, the lower layers of the model are well trained to detect basic attributes of objects in images. This helps the model differentiate between various objects in the images of our video sample during the process of finetuning. After the end of model training, we ex-post identify the salient parts of images that are associated with an outcome through gradient-based activation maps (cf. Selvaraju et al., 2017). We find gradients by taking the derivative between the predicted continuous outcome (or class of predicted binary outcome) and the output of the activation layer after the last convolution layer in each VGG-16 architecture that processes one video frame. However, unlike Selvaraju et al. (2017), we do not apply the ReLU (Rectified Linear Unit) activation on the gradient values as we would like to retain negative gradient values for interpretation. Hence our approach is a modified gradient-based activation map that is suitable for our setting. Areas of the image with positive (negative) gradients correspond to regions that are positively (negatively) associated with continuous outcomes and the predicted class of loveability.

Online Appendix D – Multimodal Approach

D.1 Embeddings and Model Design

We use the state-of-the-art individual models discussed in Section 5.1 to generate embeddings from unstructured data. This makes our multimodal approach comparable with our combined model (equation (1)) that uses the predictions from the individual models in Section 5.1. Specifically, we generate embeddings from text data using the second-to-last encoder of the pre-trained BERT model (Devlin et al., 2018; Xiao, 2018), embeddings from audio data using the predictions from the pre-trained YAMNet model (Pilakal & Ellis, 2020), and embeddings from image data using the global average pooling layer of the pre-trained VGG-16 model (Simonyan & Zisserman, 2014). Specifically, these embeddings are generated in two steps: (a) we first generate an embedding from each 30-second segment (over the entire duration of a video), and (b) average the embedding over the length of each 30 second segment to get a unique vector for each segment. Hence, for each 30-second segment, we get a text embedding (averaged from the CLS to SEP token) of dimension $(n,1,768)$, audio embedding (averaged over each patch of 960 ms with hop size of 490ms) of dimension $(n,1,521)$ and image embedding (averaged over each frame at one frame per second) of dimension $(n,1,512)$, where n is the total number of videos in our sample.

Our multimodal architecture (shown earlier in Figure 4) is inspired from the work of Ghosal et al. (2018) and Wu et al. (2014). We borrow the relevant aspects of their architecture and parameter choices to our setting. Our architecture takes as input the text embeddings u_{1m} of captions/transcript, audio embeddings u_{2m} and image embeddings of video frames u_{3m} , which are of dimensions $(n,m,768)$, $(n,m,521)$ and $(n,m,512)$ respectively, where n is the number of videos in the sample and m is the number of 30-sec segments. In addition, we supply as input the set of structured features X_{it} (listed earlier in Table 2), text embeddings for title $(n,1,768)$, text embeddings for description (first 160 characters) $(n,1,768)$ and image embeddings for thumbnail $(n,1,512)$. Note that we scale each set of embeddings by their respective L^2 norm (before supplying them as input to our multimodal model) so that their relative influence is comparable. We also do this same scaling for the structured features.

We pass the set of embeddings u_{1m} , u_{2m} and u_{3m} through separate Bi-Direction GRU layers which capture the sequential interdependence between different 30-sec clips of each modality (Ghosal et al., 2018). This is followed by a sequence of dense time-distributed layers to further capture the sequential dependence from the output of the preceding layer (Ghosal et al., 2018). We follow this up with a dense transformation layer to further process the information from the preceding layer (Wu et al., 2014). Similarly, the input from the structured features and the incentive to click data (title, description and thumbnail) are passed through separate dense transformation layers to process the data (Wu et al., 2014). Hence, we have a total of seven dense transformation layers and each of them are followed by a global average pooling layer and the outputs of the seven layers are then concatenated (Ghosal et al., 2018). This

is then supplied as input to a dense fusion layer that captures interactions between all the preceding layers (Wu et al., 2014), which is then finally connected to an output layer.

D.2 Results of Multimodal Model for Relative Importance of Position in Video

Similar to our approach in Section 7.1.3 and Table 8, we test whether embeddings from the beginning 30 seconds (across text (captions/transcript), audio and images (video frames)) are significantly more important in predicting engagement than embeddings from the middle and end 30 seconds. In order to do so, we permute the embeddings from the beginning 30 seconds in the holdout sample while holding all other features constant, and measure the change in prediction error. We repeat this process for the middle and end 30s. Subsequently, we compare the difference in prediction errors between the permuted positional embeddings across 50 bootstrap iterations using a t-test and show the difference in means in Table D1. We find that the beginning 30s is significantly more important than middle or end 30s (*as there is an increase in RMSE or decrease in accuracy*) while predicting each of our engagement measures, consistent with the findings for the Combined Model in Table 7. This demonstrates that our findings hold true even when we account for interactions between modalities during the training process. Note that the difference in means between middle 30s and end 30s is minimal, and hence we do not report those results.

	Commentability	Loveability	Thumbsability	Likeability
Permuted Prediction Error: Begin 30s	0.96	0.57	0.77	0.97
Permuted Prediction Error: Middle 30s	0.86	0.65	0.73	0.93
Permuted Prediction Error: End 30s	0.86	0.67	0.72	0.95
Difference in Permuted Prediction Error: Begin 30s vs Middle 30s	0.10***	(-)0.08***	0.04***	0.04***
Difference in Permuted Prediction Error: Begin 30s vs End 30s	0.10***	(-)0.09***	0.04***	0.02***
Note: ***p<0.001				

Table D1: Results of Multimodal Model for Position (Embeddings from Begin, Middle and End 30s) (RMSE for commentability, thumbsability and likeability; Accuracy for loveability)

Online Appendix E – Feature Generation of Theory-based Features

We generate theory-based features with the help of trusted databases, reliable transfer learned models and accurate APIs, which is more efficient as compared to employing human coders. We elaborate on this below.

For text data, as discussed in 3.3.1, we focus on the following features: presence of brand mentions and emotional words in captions/transcript³ in 30 seconds of the beginning, middle and end of a video. We identify these features by applying *regular expressions* on textual data while relying on a master list of words. The master list of brand names comprise the Top 100 Global brands in 2019 that were obtained from BrandZ, Fortune100 and Interbrand. We then add more than 32,000 brands (with US offices) from the Winmo database to this list. This is further combined with brand names identified by applying Google’s Vision API - Brand Logo Detection on thumbnails and video frames (one fps in 30 seconds of beginning, middle and end) in our sample. From this combined list, we remove more than 800 generic brand names such as ‘Slice,’ ‘Basic,’ ‘Promise,’ etc. that are likely to be used in non-brand related contexts. The master list of emotional words is obtained from the list of 2,469 emotional words identified in the LIWC dictionary (Berger & Milkman, 2012; Pennebaker et al., 2015). We identify brand and emotion mentions within 305,554 word-pieces that are generated by the BERT model using captions/transcript across all parts (beginning, middle and end) of the 1620 videos in our sample. We find that 28% (80%) of videos have a brand (emotion) mentioned at least once (in any part of the video).

For audio data, as discussed in 3.3.2, we mainly focus on the following features: music and human speech in 30 seconds of the beginning, middle and end of a video. The YAMNet model (Mel Spectrogram + MobileNet v1) finds the predicted probability of each moment⁴ of a 30 second audio clip (which has 60 moments) belonging to a sound class. Our model can efficiently accomplish this identification for 291,600 moments (1620 videos x 3 parts x 60 moments in a part). We combine the identified sound classes into different categories based on the AudioSet ontology (Gemmeke et al., 2017) – *Human* (86%), *Music* (83%), *Animal* (17%), and *Others* which include sounds of silence, things, ambiguous sounds, background sounds and natural sounds. The percentage in brackets indicates the percentage of videos that contain a sound of that category (with probability > 0.5) in any part of the video. Note that a moment of sound can be classified into multiple categories if sounds from more than one category occur together.

³ We do not study features within unstructured data that are visible in search engine results such as title or description (and thumbnail), because such unstructured data are visible before a video starts playing and hence help promote views. Our engagement measures, on the other hand, control for the number of views.

⁴ Each moment is 960ms long, and the subsequent moment begins after a hop of 490ms. Hence, each 30 second audio clip encompasses 60 moments (details in Online Appendix B).

For image data, as discussed in 3.3.3, we focus on the following features: size of humans, size of face of humans, size of packaged goods, size of animals, and human facial expressions of joy and surprise. In addition, we also study the role of brand logos, and control for the size of everyday objects such as clothes & accessories and home & kitchen items. We study these features in 30 frames that lie in 30 seconds of the beginning, middle and end of a video. We identify these features using the Cloud Vision API from Google, that has been pre-trained on millions of images and whose high accuracy has been validated in prior academic and industry research (FileStack, 2019; Li & Xie, 2020; Szegedy et al., 2016). We can efficiently implement this API over 145,800 frames (1620 video x 3 parts of video x 30 frames per part). The API returns the vertices of the identified object which allows us to create a rectangular bounding box to define its area. We divide the identified objects into eight different categories – *Humans* (91%), *Faces* (86%), *Animals* (27%), *Brand Logos* (16%), *Packaged Goods* (28%), *Clothes & Accessories* (86%), *Home & Kitchen* (58%), and *Other Objects*. The percentage in brackets indicate the percentage of videos that contain an object of that category (in any part of the video). The API also returns the level of surprise or joy in each face that was detected: {-2: very unlikely, -1: unlikely, 0: possible, 1: likely, 2: very likely}.

Online Appendix F – Comparison of Model Performance

We compare the predictive performance of our individual models for Text, Audio and Images with standard benchmarks used in the marketing literature to demonstrate that our models do not compromise on predictive ability.¹ To make this comparison, we choose the two outcome measures of deep engagement: commentability (continuous outcome) and loveability (binary outcome). For the unstructured covariates, we focus on the beginning 30 seconds of video data (Tables F1, F2 and F3) in addition to title (Table F1), description (first 160 characters) (Table F1) and thumbnails (Table F3).

We first compare the predictive performance of the Text Model (BERT) with four standard models in Table F1. These standard benchmarks include an LSTM (with a 300 dimensional Glove word vector embedding), CNN model (Liu et al., 2019), CNN-LSTM (Chakraborty et al., 2022) and CNN-Bi-LSTM. As can be seen in Table F1, BERT performs better than the benchmarks while predicting both commentability (lowest RMSE) and loveability (highest accuracy). This is because of primarily three reasons: (1) BERT learns contextual embeddings (e.g., the embedding for the word ‘bark’ will change based on the context in which it used – a dog’s bark or tree’s outer layer) as compared to benchmarks methods which use fixed word embeddings such as Glove and word2vec (2) The entire BERT model with hierarchical layers is pre-trained whereas conventional models only initialize the first layer with a word embedding (3) BERT uses a self-attention mechanism that avoids loss of information as compared to a sequential process (such as in an LSTM) that can lead to loss of information.

Outcome	Covariate	LSTM	CNN	CNN-LSTM	CNN-Bi-LSTM	BERT
Commentability	Title	0.99	0.91	0.90	0.88	0.83
	Description (first 160c)	0.98	0.93	0.89	0.88	0.87
	Captions/transcript (beginning 30s)	0.97	1.04	0.94	0.93	0.92
Loveability	Title	0.67	0.70	0.70	0.70	0.72
	Description (first 160c)	0.50	0.69	0.69	0.69	0.70
	Captions/transcript (beginning 30s)	0.67	0.70	0.70	0.70	0.71

Table F1: Comparison of Text Model predictive performance on holdout sample for measures of deep engagement (RMSE for commentability; Accuracy for loveability)

We now compare the model performance of the Audio model with other variants that are devoid of transfer learning and attention, and present the results in Table F2. First, we find that the addition of the transfer learned MobileNet v1 to a model that uses only the Mel Spectrogram + Bi-LSTM results in improved RMSE when predicting commentability and improved accuracy when predicting loveability.

¹ We run all the standard benchmark models at least three times and average their prediction errors. We run our main models for Text and Audio (and Image) 50 (and 25) times and average their prediction errors.

Addition of the attention mechanism to this results in our Audio model. However, this does not improve the prediction error but also does not deteriorate it. Overall, our Audio model performs the best in out-of-sample prediction, thus demonstrating that transfer learning (via MobileNet v1) contributes towards the predictive ability of the model. Also, capturing relative attention weights (via the attention mechanism) while contributing towards interpretability does not deteriorate predictive ability.

Outcome	Covariate	Mel Spectrogram + Bi-LSTM	Mel Spectrogram + MobileNet v1 + Bi-LSTM	Audio Model: Mel Spectrogram + MobileNet v1 + Bi-LSTM + Attention
Commentability	Audio (first 30s)	0.95	0.92	0.92
Loveability	Audio (first 30s)	0.59	0.64	0.64

Table F2: Comparison of Audio Model performance on holdout sample (RMSE for commentability; Accuracy for loveability)

Next, in Table F3, we compare the performance of the Image Model (VGG-16) with a simple 4-layer CNN model using thumbnail data. We see a substantial improvement in both RMSE and accuracy when using VGG-16, thus demonstrating the benefits of both transfer learning and a deeper architecture.

Outcome	Covariate	4-layer CNN	VGG-16
Commentability	Thumbnail	2.53	0.96
Loveability	Thumbnail	0.55	0.68

Table F3: Comparison of Image Model performance on holdout sample (RMSE for commentability; Accuracy for loveability)

Online Appendix G – Details of Interpreting Text Model Results

G.1 Modelling Choice of Ridge Regression

We use Ridge Regression to interpret the relationships captured in the Text Model so that we can capture heterogeneity in effects across brands and emotional words. Additional reasons for our choice of Ridge Regression are as follows: (a) Some brands or emotional words may only be used once in our data and hence OLS cannot be used, (b) number of predictors $n_p > n$ for Eq (5) while interpreting the Text model, which makes Ridge Regression suitable, and (c) a limitation of other penalized regression methods such as LASSO is that it will cap variable selection at n variables (and not n_p) and hence we may miss out on capturing important predictors, (d) LASSO or Elastic Net may miss out on selecting some brands or emotional words if their effect is collinear with other brands or emotional words, (e) Ridge Regression shrinks the non-important predictors towards 0, thus allowing us to identify the relatively more important predictors.

G.2 Graphical Illustration and Robustness of Interpretation Results of Text Model

We show a graphical illustration of the findings highlighted in green in Table 9 in Figure G1. The X axis shows the median value of brand coefficients (across 50 bootstrap iterations) from Step 1 of the analysis that correspond to a change in the attention weights. The Y axis shows the median value of brand coefficients (across 50 bootstrap iterations) from Step 2 of the analysis that correspond to a change in the predicted outcome. Our quadrants of interest are Quadrant 1 and 4 that have a positive X axis corresponding to an increase in attention directed to the brand/emotion. The brands/emotions in Quadrant 1 have a positive Y axis corresponding to an increase in the predicted outcome variable, whereas those in Quadrant 4 have a negative Y axis corresponding to a decrease in the predicted outcome variable. We label the data points for the brands/emotions in these quadrants whose coefficient value is at least 30% (*bar* value) of the magnitude of the maximum coefficient value on each axis to avoid cluttering the figures with labels (Note that the results in Table 9 used a *bar* of 5%). The values in brackets below the name of a brand in Q1 (Q4) correspond to the % of time (across 50 bootstrap iterations) the brand coefficient is positive (positive) on the X axis and positive (negative) on the Y axis. As can be seen in the graph, brands are more often present in Q4 as compared to Q1.

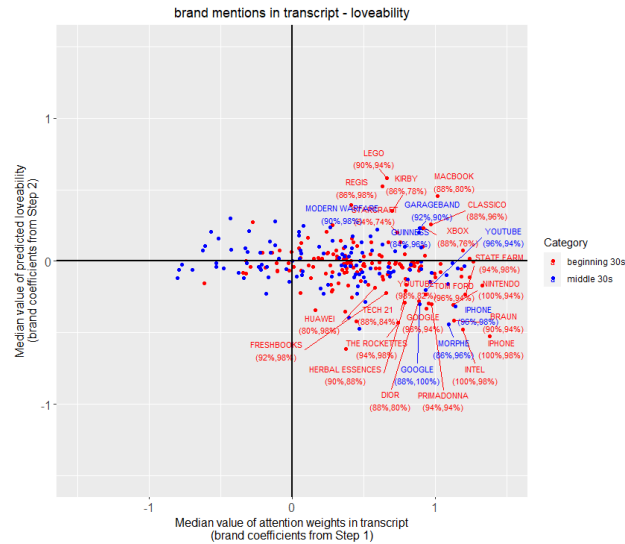


Figure G1: Interpretation results of Text Model for brand mentions

The results for the Text model corresponding to the highlighted cells in green in Table 9 are robust to changes in the values of the *bar*. This is because the difference between the percentage of brands that have a negative effect (Quadrant 4) versus a positive effect (Quadrant 1) on predicted loveability continue to hold true across a range of values of the *bar*. We show this in Figure G2. As can be seen, the green and brown lines do not intersect which demonstrates that the differential effect is in the same direction as we move along the respective X and Y axis of Figure G1. In other words, we demonstrate how our findings for the beginning 30s and middle 30s are robust to brands that have a small or a large effect on predicted loveability.

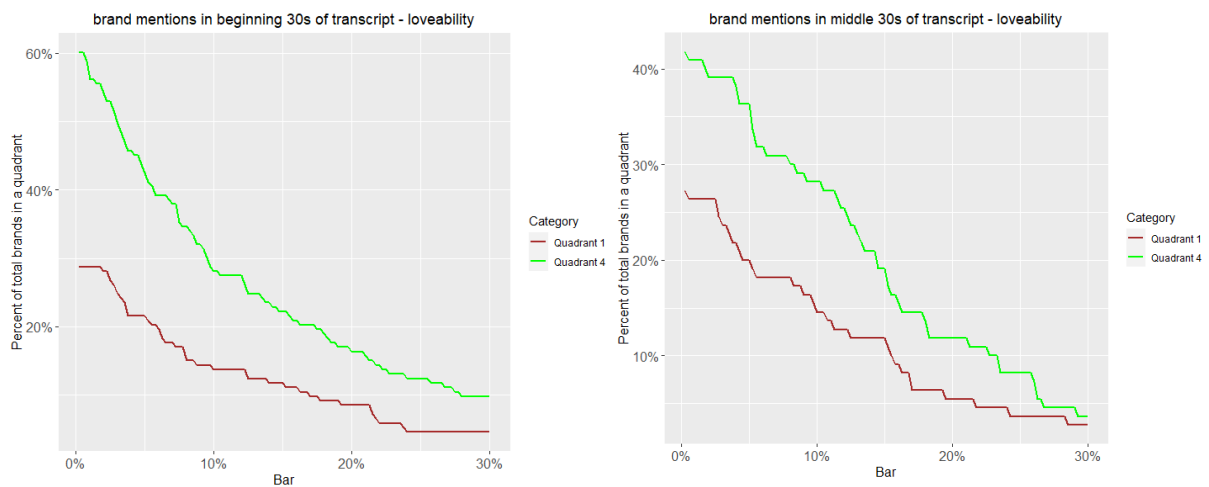


Figure G2: Robustness of interpretation results of Text Model for brand mentions in beginning 30 seconds and middle 30 seconds

G.3 Modelling Choice of OLS

We are able to estimate Eq (5) using OLS while modeling the predicted outcomes from the Audio or Image models because in these instances we do not model the heterogeneity across brands or emotional words. Instead, we use covariates for ‘number of brand mentions’ and ‘number of emotional word mentions’ because textual features in this case are not features of interest and are only used as controls.

More concretely, we replace $\sum_{k=1}^{n_b} \beta_{1pk}(BITX_{it}) + \sum_{k=1}^{n_e} \beta_{2pk}(EITX_{it})$ in Eq (5) with $\beta_{1p}(\text{Number of brand mentions}_{it}) + \beta_{2p}(\text{Number of emotion mentions}_{it})$.

Online Appendix H – Simulations to Recover the True Data Generating Process

We explain in detail our simulation process for the Text Model in H.1, Audio Model in H.2 and Image Model in H.3.

H.1 Simulations – Text Model

We first pick a covariate-outcome pair of interest, say “brand mentions in beginning 30 seconds of captions/transcript – likeability”. For those observations (of video t and influencer i) where a brand is *not* mentioned in the beginning 30 seconds, we generate a random normal distribution of log-likeability whose mean and standard deviation match the observed mean and standard deviation of our entire sample:

$$brand_absent_{it} \sim N(3.79, 1.11)$$

For those observations (of video t and influencer i) where a brand is mentioned in the beginning 30 seconds, we generate a random normal distribution of log-likeability whose mean is twice the mean and standard deviation is half the standard deviation of the above equation:

$$brand_present_{it} \sim N\left(2 * 3.79, \frac{1.11}{2}\right)$$

We can summarize our simulated outcome of log likeability, $Y_{simulated_{it}}$, for video t by influencer i , as follows:

$$Y_{simulated_{it}} = \begin{cases} N(3.79, 1.11) & \text{when brand is absent} \\ N\left(2 * 3.79, \frac{1.11}{2}\right) & \text{when brand is present} \end{cases}$$

We visually illustrate the results of ex-post interpretation in Figure H1. As can be seen in the figure, brands are more often present in Quadrant 1 (increase in attention and an increase in predicted likeability). The results for the Text model are also robust to changes in the value of the *bar* used in Table 14. This is because the difference between the percentage of brands that have a positive effect (Quadrant 1) versus a negative effect (Quadrant 4) on predicted likeability continue to hold true across a range of values of the *bar*. We show this in Figure H2. As can be seen, the green and brown lines do not intersect which demonstrates that the differential effect is in the same direction as we move along the respective X and Y axis of Figure H1. Hence, our findings are robust to brands that have a small or a large effect on predicted likeability.

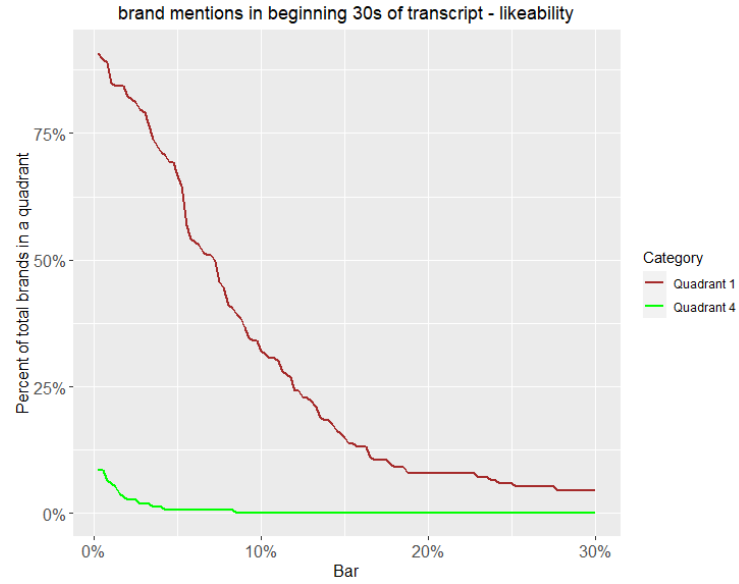
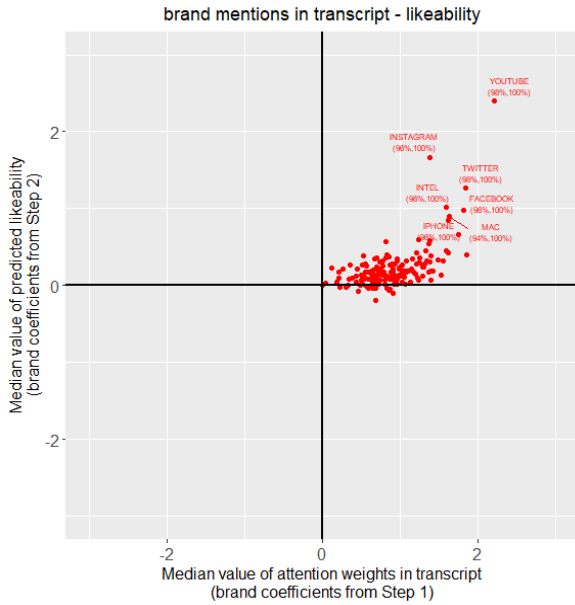


Figure H1: Interpretation Results of Simulation – Text Model

Figure H2: Robustness of Interpretation Results of Simulation – Text Model

H.2 Simulations – Audio Model

As done above, we first pick a covariate-outcome pair of interest, say “music duration in beginning 30 seconds – commentability”. We then generate a random normal distribution of log-commentability (for video t by influencer i) whose minimum and maximum value match the observed minimum and maximum values in our entire sample:

$$v_{it} \sim \text{Uniform}(-11.42, -2.18)$$

We then generate the simulated outcome of log commentability, $Y_{simulated_{it}}$, for video t by influencer i as follows:

$$Y_{simulated_{it}} = v_{it} - 0.5 * \text{Sum of } CI(\text{Music})_{it}$$

where, $\text{Sum of } CI(\text{Music})_{it}$ is the duration of music sounds in the beginning 30 seconds in video t by influencer i .

H.3 Simulations – Image Model

As done above, we first pick a covariate-outcome pair of interest, say “size of human images in beginning 30 seconds – likeability”. We then generate a random normal distribution of log-likeability (for video t by

influencer i) whose minimum and maximum value match the observed minimum and maximum values in our entire sample:

$$w_{it} \sim \text{Uniform}(-0.92, 6.83)$$

We then generate the simulated outcome of log likeability, $Y_{\text{simulated}_{it}}$, for video t by influencer i as follows:

$$Y_{\text{simulated}_{it}} = w_{it} + 0.25 * \text{SizeObject}(\text{Human})_{it}$$

where, $\text{SizeObject}(\text{Human})_{it}$ is the mean across 30 frames of the percentage of the image occupied by all objects that are human images in video t made by influencer i .

Online Appendix I – Detailed Managerial Implications

We discuss detailed implications of our research. In I.1, we discuss a video scoring mechanism that can be used by influencers to score a video and identify areas for improvement. Similarly, in I.2 we show how importance measures (attention weights for text and audio; and gradients for images) can be visualized to help influencers identify areas for improvement. In I.3, we decompose the variance explained by brand mentions while predicting loveability, so that marketers and brands can understand the overall impact of branded content in influencer videos.

I.1 Video Scoring Mechanism

Marketers may be interested in evaluating influencer videos in a holistic manner. We develop a video scoring mechanism using Partial Dependence Plot (PDP) (Friedman, 2001) to help them determine the influence of unstructured components in influencer videos.

A video can be scored out of 100% on each of its unstructured elements when predicting any of the engagement measures. We do this with the help of the combined Ridge Regression model shown in equation (1) in the main manuscript. We begin by creating a linear Partial Dependence Plot (PDP) (Friedman, 2001) between $\hat{Y}_{it<unstructured>}$ and Y_{it} in the training sample, where the value of $\hat{Y}_{it<unstructured>}$ is the average across all bootstrap iterations (as done earlier in Section 7.1). We note the values of $\hat{Y}_{it<unstructured>}$ that correspond to a minimum and a maximum change in the predicted outcome. We then note the values of $\hat{Y}_{it<unstructured>}$ for a random video in the holdout sample. We scale it using min-max scaling to get a score out of 100% for each unstructured element while predicting each outcome. Finally, we get an overall score by weighing the score for each unstructured element with its relative importance score (found earlier in Table 7 - Panel A).

As an illustration, let us take the point of view of a brand that is evaluating a particular influencer as a potential partner. As a sample, they pick this video (https://www.youtube.com/watch?v=3-oWqeA_hc4) and score it as above which is shown in Table II. We can see that the video's weakest performance area based on its overall score is on both its engagement levels – commentability (30.6%) and thumbsability (48.5%) – and the corresponding weakest elements are captions/transcript in the beginning 30 seconds (10.1%) and audio in the middle 30 seconds (26.0%) respectively. Brands and agencies can use these scores to suggest areas of improvement to influencers, and compare scores of this video to scores from other videos of the same or a different influencer. These scores can be used in conjunction with the visualization techniques described in I.2 to help influencers identify areas for improvement. Influencers can use these scores to progressively refine their videos for the relevant engagement measure that is of concern to them or the brand partner. Note that these summary scores are based on correlations between video elements and engagement, so their value lies in providing directions

along which improvements are most likely. In contrast, without these scores, the number of directions on which influencers and brands can work is very large.

		Deep Engagement		Shallow Engagement	
		Loveability	Commentability	Likeability	Thumbsability
Incentive to Click features	Title	100.0%	23.9%	75.1%	51.5%
	Description (first 160c)	100.0%	34.0%	73.5%	62.7%
	Thumbnail	0.0%	87.5%	46.3%	26.5%
Captions/ Transcript	Begin 30s	100.0%	10.1%	76.6%	44.0%
	Middle 30s	100.0%	25.7%	80.7%	50.5%
	End 30s	100.0%	24.2%	88.2%	50.5%
Audio	Begin 30s	0.0%	83.6%	48.9%	26.7%
	Middle 30s	0.0%	19.5%	72.9%	26.0%
	End 30s	100.0%	67.0%	57.6%	31.9%
Video Frames	Begin 30s	100.0%	45.2%	63.6%	62.7%
	Middle 30s	0.0%	23.0%	49.0%	28.6%
	End 30s	100.0%	60.9%	69.0%	59.2%
Overall Score		93.6%	30.6%	72.9%	48.5%
	Observed value for video	Positive	6 comments per 10K views	118 likes per dislike	181 likes or dislikes per 10K views

Table 11: Score for a random influencer video outside the training sample

I.2 Visual Illustration of Salient Regions in Text, Audio and Images

We discuss the process to visualize salient regions in unstructured data based on the results of our models in Section 7.2. These techniques can help influencers identify potential areas for improvement.

We illustrate an example of how text data can be visually interpreted. In Figure 11, we show the attentions weights on the captions/transcript (first 30s) from a video of a technology & business influencer. The words are tokenized into word-pieces in the figure as done by the model, and a darker background color indicates relatively higher attention weights. As can be seen in the figure, on average more attention is paid to the word ‘iphone’ than other words in the text. Note that the model assigns different attention weights to the word ‘the’ based on the context in which it is used (lower attention in the first line, but higher attention in the last line). While the model also assigns more attention to punctuation marks, such as the apostrophe, these associations may be spurious (as discussed earlier in Section 6) or may be confounded by word usage unique to the influencer which we control for during ex-post interpretation using influencer fixed effects (α_i) in equation (2). Our model predicts ‘not positive’ loveability for this clip (consistent with the findings in Table 9) and this matches the observed value.

what is up guys lew here and this is the iphone 5 camera test if you haven't subscribed yet definitely click that button right now so you don't miss out on any of my iphone 5 coverage or tests there is a button around you find it click it anyway this video here we're going to be looking at the rear facing camera as well as the newly improved forward facing camera which now shoot 720p making it a viable option for shooting vlogs and things like that stick around till the end of the video to get all

Figure 11: Attention weights in captions/transcript (first 30s) of a video

Next, we illustrate an example of how attention paid to audio moments in a video can be visually interpreted. We focus on the relationship between music and loveability. In Figure I2, we show the first 30 seconds of the audio clip of a travel influencer using four sub plots. The first plot shows the variations in the amplitude of the 30 second audio wave (sampled at 16 KHz) followed by the spectrogram of the wave where brighter regions correspond to stronger (or louder) amplitudes. Next, we show the interim output of the Audio model with the top 10 sound classes at each moment in the audio, where the darker squares indicate higher probability of observing a sound of that class at that moment. The last plot displays the attention weights corresponding to each moment in the audio clip, where the darker squares indicate higher relative attention placed on that moment while forming an association with loveability. As can be seen in the figure, relatively more attention is directed to moments where there is music but no simultaneous speech. The model predicts positive loveability for this clip (consistent with the findings in Table 10) and this matches the observed value.

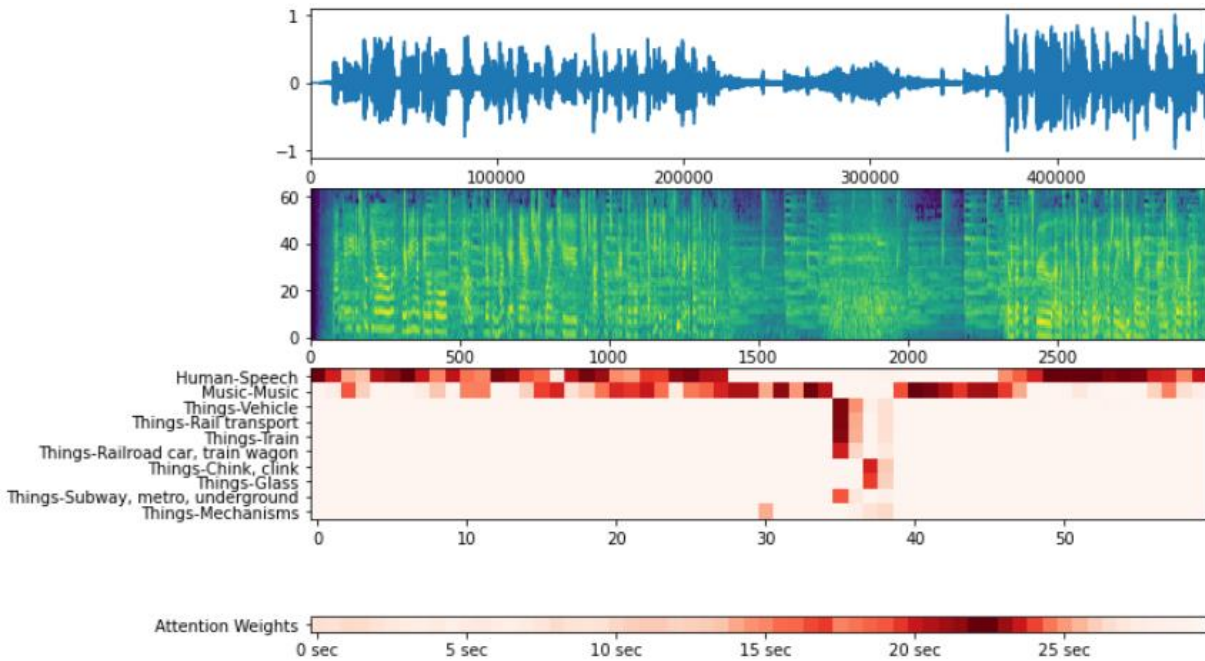


Figure I2: Attention weights in an audio clip (first 30 sec) of a video

Next, we illustrate how attention paid to image pixels on the video frames of a video can be visually interpreted. We show the first 15 frames @1fps for a video of a parenting influencer in Figure 13. The bottom of the figure shows the heat map (gradient values), where brighter (redder) regions are positively associated with likeability. We find that pixels associated with images of persons have brighter heat maps, and more attention is often paid to the whole image of the person than just the face of the person (e.g., Frame 3, 5, 6 and 7). This is correlated with the area below the face of the person where the influencer is gesturing with their hands. We can also note the attention paid to images of packaged goods in Frame 14 and 15. Also note that the model assigns high attention to all the pixels in Frames 1, 9 and 13, and hence they appear completely red. The predicted likeability for this example is 40 likes per dislike which is less than the median likeability of 54 likes per dislike. This can be expected given that the person is present in only around half the frames and the large size of packaged goods in the frames (which is consistent with the conclusions from Table 11).

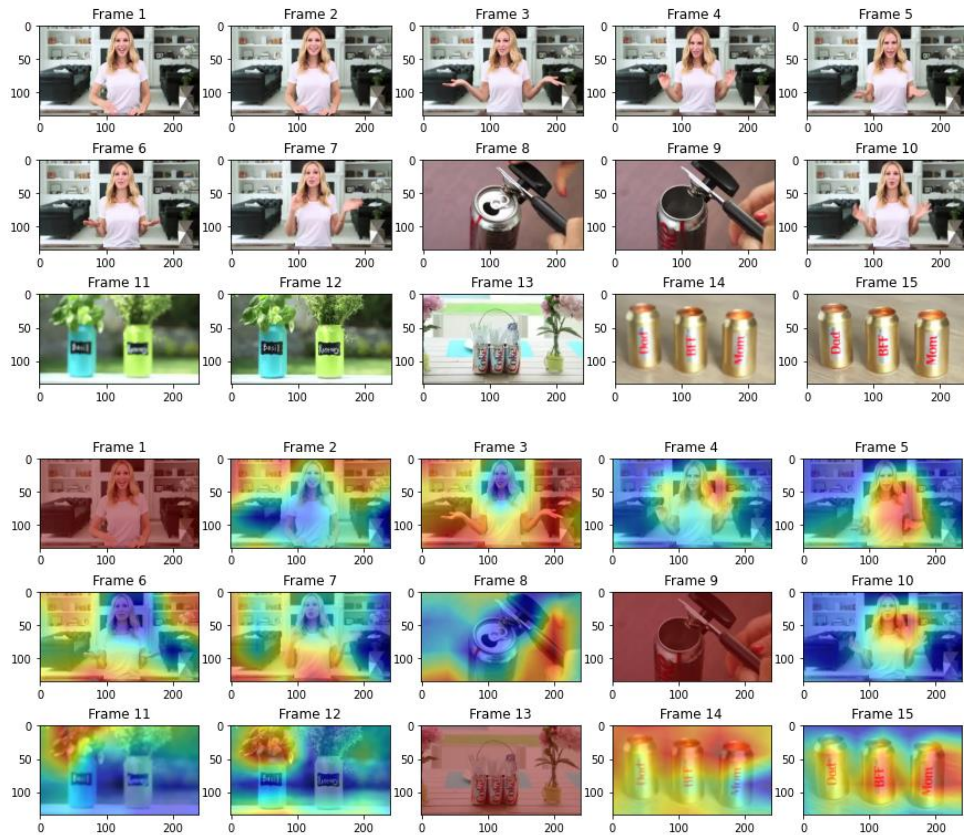


Figure 13: Gradient heat map in video frames (first 15 seconds) of a video

These visual illustrations for text, audio and images can help influencers and brand partners understand the potential influence of individual words, sound elements and objects in images. It can help them experiment with usage of different words, sounds and objects that can improve engagement with the video.

I.3 Decomposing Variance Explained by Brand Mentions

A bigger question for marketers is to understand the overall importance of branded content in these influencer videos. One way to quantify this is to decompose the variance explained by brand related content in the relationship between a covariate-outcome pair. We decompose the variance explained by brand mentions in the relationship between captions/transcript in the beginning 30 seconds and loveability, and show the results in Table I2. We use the Ridge Regression model (used to interpret the Text Model in 7.2.1) to measure the ability of individual brands to predict the engagement measure. As shown in the table, we calculate the improvement in prediction performance over a standard baseline which is a prediction accuracy of 50% (random chance). We find that brand mentions in the beginning 30s explain perform 10% better than chance in predicting loveability. This demonstrates that brand mentions have a small but substantial role to play in explaining the behavior of the sentiment of deep engagement. In the table, we also show the comparative performance of the Text model (BERT) (from Table 5). We find that the improvement in prediction error from using captions/transcript (beginning 30 sec) is 310% compared to only using brand mentions. This demonstrates that words other than brand names in captions/transcript (beginning 30 sec) explain a lot more variation in loveability than brand names alone.

Model	Outcome	Covariate	Holdout prediction error: $\sqrt{\frac{SSE}{n}}$ or accuracy	Holdout baseline: $\sqrt{\frac{SST}{n}}$ or chance accuracy	Percentage improvement over baseline (variance explained)	Relative performance improvement
Ridge Reg	Loveability	Individual indicators for each brand’s mention in beginning 30s	56%	50%	10%	310%
BERT	Loveability	Captions/Transcript in beginning 30s	71%	50%	41%	

Table I2: Variance explained by brand mentions

References to Online Appendix

- Alammar, J. (2018, June 27). *The Illustrated Transformer*. <http://jalammar.github.io/illustrated-transformer/>
- Bahdanau, D., Cho, K., & Bengio, Y. (2014). Neural machine translation by jointly learning to align and translate. *arXiv preprint arXiv:1409.0473*.
- Berger, J., & Milkman, K. L. (2012). What makes online content viral? *Journal of Marketing Research*, 49(2), 192-205.
- Chakraborty, I., Kim, M., & Sudhir, K. (2022). Attribute sentiment scoring with online text reviews: Accounting for language structure and missing attributes. *Journal of Marketing Research*, 59(3), 600-622.
- Devlin, J., Chang, M.-W., Lee, K., & Toutanova, K. (2018). Bert: Pre-training of deep bidirectional transformers for language understanding. *arXiv preprint arXiv:1810.04805*.
- FileStack. (2019). *Comparing Image Tagging Services: Google Vision, Microsoft Cognitive Services, Amazon Rekognition and Clarifai*. Retrieved April 25 from <https://blog.filestack.com/thoughts-and-knowledge/comparing-google-vision-microsoft-cognitive-amazon-rekognition-clarifai/>
- Friedman, J. (2001). Greedy function approximation: a gradient boosting machine. *Annals of statistics*, 1189-1232.
- Gemmeke, J. F., Ellis, D. P., Freedman, D., Jansen, A., Lawrence, W., Moore, R. C., Plakal, M., & Ritter, M. (2017). Audio set: An ontology and human-labeled dataset for audio events. 2017 IEEE International Conference on Acoustics, Speech and Signal Processing (ICASSP),
- Gers, F. A., Schmidhuber, J., & Cummins, F. (1999). Learning to forget: Continual prediction with LSTM.
- Ghosal, D., Akhtar, M. S., Chauhan, D., Poria, S., Ekbal, A., & Bhattacharyya, P. (2018). Contextual inter-modal attention for multi-modal sentiment analysis. proceedings of the 2018 conference on empirical methods in natural language processing,
- Howard, A. G., Zhu, M., Chen, B., Kalenichenko, D., Wang, W., Weyand, T., Andreetto, M., & Adam, H. (2017). Mobilenets: Efficient convolutional neural networks for mobile vision applications. *arXiv preprint arXiv:1704.04861*.
- Krizhevsky, A., Sutskever, I., & Hinton, G. E. (2012). Imagenet classification with deep convolutional neural networks. *Advances in neural information processing systems*, 25.
- Li, Y., & Xie, Y. (2020). Is a picture worth a thousand words? An empirical study of image content and social media engagement. *Journal of Marketing Research*, 57(1), 1-19.
- Liu, X., Lee, D., & Srinivasan, K. (2019). Large-scale cross-category analysis of consumer review content on sales conversion leveraging deep learning. *Journal of Marketing Research*, 56(6), 918-943.
- Pennebaker, J. W., Boyd, R. L., Jordan, K., & Blackburn, K. (2015). *The development and psychometric properties of LIWC2015*.
- Pilakal, M., & Ellis, D. (2020). *YAMNet*. <https://github.com/tensorflow/models/tree/master/research/audioset/yamnet>
- Selvaraju, R. R., Cogswell, M., Das, A., Vedantam, R., Parikh, D., & Batra, D. (2017). Grad-cam: Visual explanations from deep networks via gradient-based localization. Proceedings of the IEEE international conference on computer vision,
- Simonyan, K., & Zisserman, A. (2014). Very deep convolutional networks for large-scale image recognition. *arXiv preprint arXiv:1409.1556*.
- Szegedy, C., Vanhoucke, V., Ioffe, S., Shlens, J., & Wojna, Z. (2016). Rethinking the inception architecture for computer vision. Proceedings of the IEEE conference on computer vision and pattern recognition,
- Widex. (2016, August 9). *The human hearing range - what can you hear?* <https://www.widex.com/en-us/blog/human-hearing-range-what-can-you-hear>
- Wu, Y., Schuster, M., Chen, Z., Le, Q. V., Norouzi, M., Macherey, W., Krikun, M., Cao, Y., Gao, Q., & Macherey, K. (2016). Google's neural machine translation system: Bridging the gap between human and machine translation. *arXiv preprint arXiv:1609.08144*.
- Wu, Z., Jiang, Y.-G., Wang, J., Pu, J., & Xue, X. (2014). Exploring inter-feature and inter-class relationships with deep neural networks for video classification. Proceedings of the 22nd ACM international conference on Multimedia,
- Xiao, H. (2018). *BERT-as-service*. <https://bert-as-service.readthedocs.io/en/latest/section/faq.html#why-not-the-last-hidden-layer-why-second-to-last>
- Yue-Hei Ng, J., Hausknecht, M., Vijayanarasimhan, S., Vinyals, O., Monga, R., & Toderici, G. (2015). Beyond short snippets: Deep networks for video classification. *Proceedings of the IEEE conference on computer vision and pattern recognition*, 4694-4702.